

# Development of techniques for measuring the mobility of knee joints in children with Cerebral Palsy

Louise Wrange & Nadia Wåhlin  
Lund, February 2018



**LUND**  
UNIVERSITY

Master's Thesis in  
Biomedical Engineering

Faculty of Engineering LTH  
Department of Biomedical Engineering

Supervisor: Ingrid Svensson  
Assistant supervisor: Nebojsa Malesevic



# Acknowledgements

First and foremost, we would like to extend our gratitude to our supervisor Ingrid Svensson and assistant supervisor Nebojsa Malesevic who shared their knowledge, helped and supported us throughout this project.

Another person we would like to thank is Gunnar Hägglund, professor in orthopedics, who proposed this subject for our thesis and who always showed enthusiasm for this project.

We would also like to thank the staff at the department of Biomedical Engineering for making us feel at home and providing us with coffee and breakfast on Fridays. The Christmas train serving gingerbread cookies and marshmallow Santas in the lunch room was epic.

And lastly, a thank you to our families for their love and support and to our second families, Spegatspexet and Var GladSpexarna, for boosting our moods.



---

*I shot through my twenties like a luminous thread through a dark needle, blazing toward my destination: Nowhere.*

*Carrie Fisher*



# Abstract

Cerebral Palsy, commonly referred to as CP, is a neurological disorder that results in loss or impairment of motor function, which affects body movement, muscle control, muscle coordination and balance. In Sweden, about 200 children are diagnosed with Cerebral Palsy every year and the disorder can cause imbalances between the muscles. These imbalances can lead to contractures which is equivalent to permanent shortening of muscles and stiffness of joints. This can severely affect the mobility of the child and the quality of life.

Today, the only way for physicians or physiotherapists to evaluate the movement of the joints, is during a patient's short visits to the hospital. The purpose of this project was to develop a device that was able to measure the range of motion of the knee during a longer period of time, which could help customize the child's rehabilitation.

The initial approach was to implement two inertial measurement units (IMUs) and find the angle between the sensors. Different solutions on finding the angle was tested without being able to obtain stable data and the project members chose a new approach.

Instead of IMUs, a potentiometer was used and stable data was obtained. A prototype was developed in an iterative and incremental product development process and data was collected during different types of physical exercise.

The final prototype was wireless, able to collect data during ordinary life activities and had a battery life of over 30 hours. The data was analyzed and the results were accurate but showed that the prototype probably hindered some of the natural movement of the knee. The developed prototype is a step towards being able to measure the knee range of motion during a longer period of time, and could be a tool for physicians and other medical staff when evaluating and rehabilitating children with CP.

# Sammanfattning

Cerebral pares (CP) är en neurologisk störning som kan leda till förlust eller nedsättning av de motoriska funktioner som påverkar kroppens rörelser, muskelkontroll, muskelkoordinering och balans.

I Sverige diagnostiseras cirka 200 barn varje år med CP, som kan orsaka obalanser mellan musklerna. Dessa obalanser kan leda till kontrakturer, som motsvarar en permanent förkortning av musklerna och ökad styvhet i lederna. Muskelförkortning och ledstyvhet kan drastiskt påverka barnets rörlighet och därmed även livskvaliteten.

Idag är det enda sättet för läkaren eller fysioterapeuten att utvärdera barnens rörelsefunktion under kortare besök på sjukhuset. Därför var syftet med detta projekt att utveckla en prototyp som kunde mäta knäets ledrörlighet under en längre period.

Det första tillvägagångssättet var att använda två inertial measurement units (IMU) och hitta vinkeln mellan dessa två sensorer. Trots olika försök av att implementera sensorerna så lyckades projektmedlemmarna inte erhålla stabil data och valde därför ett nytt tillvägagångssätt.

Istället användes en potentiometer för att utveckla en metod för att erhålla vinkeln. En prototyp utvecklades under en iterativ och inkrementell process och data samlades in under olika typer av fysisk rörelse.

Den slutgiltiga prototypen var trådlös, kunde samla in data och hade en batteritid på över 30 timmar. Data från prototypen analyserades och resultatet var godtagbart men indikerade att prototypen förmodligen förhindrade en del av knäets naturliga rörelse.

Prototypen som utvecklats i detta projekt är ett steg mot att kunna mäta ledrörlighet under en längre tid och kan vara ett verktyg för läkare och annan medicinsk personal vid utvärdering och rehabilitering av barn med CP.



# Contents

<b>Abstract</b>	<b>iv</b>
<b>Sammanfattning</b>	<b>v</b>
<b>1 Introduction</b>	<b>2</b>
1.1 Overall objective . . . . .	2
1.2 Disposition . . . . .	3
<b>2 Background</b>	<b>4</b>
2.1 Cerebral Palsy in children . . . . .	4
2.1.1 Causes . . . . .	5
2.1.2 Characteristics and symptoms . . . . .	5
2.1.3 CPUP . . . . .	9
2.1.4 Clinical examination and treatment . . . . .	9
2.2 The knee joint . . . . .	10
2.2.1 Bones and muscles around the knee joint . . . . .	10
2.2.2 Flexion and extension of the knee joint . . . . .	10
2.2.3 Gait and flexion deformity of the knee . . . . .	12
2.3 Sensors and software . . . . .	13
2.3.1 Inertial measurement unit . . . . .	13
2.3.2 Gimbal lock . . . . .	15
2.3.3 Quaternions . . . . .	15
2.3.4 Potentiometer . . . . .	16
2.3.5 Arduino . . . . .	17
2.4 Product development process and software development . . . . .	18
2.4.1 Iterative development . . . . .	18
2.4.2 Incremental development . . . . .	18
2.4.3 General product development . . . . .	18
2.4.4 Concept development . . . . .	19
2.4.5 Identifying customer needs . . . . .	19

2.4.6	Establishing target specification . . . . .	20
2.4.7	Concept generation . . . . .	20
2.4.8	Concept selection . . . . .	20
2.4.9	Concept testing . . . . .	21
2.4.10	Setting final specifications . . . . .	21
2.5	Previous research . . . . .	21
<b>3</b>	<b>Initial information gathering</b>	<b>24</b>
3.1	Initial information gathering . . . . .	24
3.1.1	Results from initial information gathering . . . . .	25
<b>4</b>	<b>Initial specification of requirements</b>	<b>28</b>
<b>5</b>	<b>Development of IMU measurement device</b>	<b>30</b>
5.1	Initial implementation of the IMU sensors . . . . .	30
5.1.1	Results from the initial implementation of the IMU sensors	33
5.2	Initial angle measurement using IMU sensors . . . . .	34
5.2.1	Results from the initial angle measurement using IMU sensors . . . . .	35
5.3	Implementing IMU sensors with absolute orientation . . . . .	37
5.3.1	Implementing a weight function using pitch, roll and heading . . . . .	37
5.3.2	Using quaternions to find the angle . . . . .	39
5.3.3	Results from implementing IMU sensors with absolute orientation . . . . .	40
<b>6</b>	<b>Development of potentiometer measurement device</b>	<b>44</b>
6.1	Initial implementation of potentiometer . . . . .	44
6.1.1	Results from initial implementation of potentiometer . . . . .	45
6.2	Developing a wireless system . . . . .	47
6.3	Developing a wearable prototype . . . . .	49
6.3.1	Target specification . . . . .	51
6.4	The first wearable prototype . . . . .	54
6.4.1	Measurements from the first wearable prototype . . . . .	54
6.4.2	Further development of the first wearable prototype . . . . .	55
<b>7</b>	<b>The final prototype</b>	<b>58</b>
7.1	Developing the final prototype . . . . .	58
7.2	Results from the final prototype . . . . .	58

<b>8</b>	<b>Discussion</b>	<b>66</b>
8.1	IMU . . . . .	66
8.2	Potentiometer . . . . .	68
8.3	Future development . . . . .	69
8.4	Ethical aspects . . . . .	70
8.5	Conclusions . . . . .	71
<b>9</b>	<b>References</b>	<b>72</b>



# 1 | Introduction

Cerebral Palsy, commonly referred to as CP, is a neurological disorder caused by brain injury or abnormal development of the brain while a child's brain is under development. This means that the neurological damage occurs before birth, during birth, or immediately after birth. The neurological disorder results in loss or impairment of motor function that affects body movement, muscle control, muscle coordination and balance. In Sweden, about 200 children are diagnosed with Cerebral Palsy every year and the disorder can cause imbalances between the muscles. These imbalances can lead to contractures which is equivalent to permanent shortening of muscles and stiffness of joints. This can severely affect the mobility of the child and the quality of life.

Today, the only way for the physician or physiotherapist to evaluate the movement of the joints, is during a patient's short visits to the hospital. If there was a way to monitor and continuously track the joint movements during a longer period, the physician or physiotherapist would acquire a more realistic and accurate description of a child's movement and mobility. Such monitoring would facilitate and improve preventative treatment.

## 1.1 Overall objective

The main objective of the project is to develop a device that can continuously measure a child's movement/range of joint motion in the knee during a prolonged time period. The device should be comfortable for the child to wear and have minimal impact on the daily life of the child.

## **1.2 Disposition**

This report will first give the reader some background information on Cerebral Palsy and the knee joint. This will be followed by a section about the sensors and software program used in this project. After that the methods of the product development process will be described followed by the initial literature search.

The next part will describe the development process and results from using IMU sensors to develop the measurement device. This will be followed by the development process and results from creating the measurement device using a potentiometer. The final prototype will then be presented in the chapter that follows. The final part of the report will include the discussion and conclusions from the project.

## 2 | Background

The following chapter will give the reader an overall view of the subject Cerebral Palsy, followed by the knee joint and its function. The later section of this chapter will treat the previous research on which this thesis is based on, follow by a description of the sensors and software used in the development process.

### 2.1 Cerebral Palsy in children

Cerebral Palsy (CP) is an umbrella term that includes childhood disorders of posture and movement, and affects the person throughout his or her life. The definition of CP is a much debated subject. There are several definitions but two of the more recent and up-to-date are presented and used in this project. In 1992, Mutch et al [1] defined CP as “an umbrella term covering a group of non-progressive, but often changing, motor impairment syndromes secondary to lesions or anomalies of the brain arising in the early stages of development”. Aisen et al [2] defined CP in 2011 as a “motor impairment that limits the activity and is often accompanied by impaired cognition, communication, and sensory perception, behavioural abnormalities, seizure disorders, or these features combined”. The term *Cerebral* refers to the cerebrum of the brain and *Palsy* refers to the loss or impairment of motor function [3]. The cerebrum is the principal and most anterior part of the brain and it is located in the front area of the skull. It consists of two hemispheres, right and left, which are separated by a fissure. The cerebrum is responsible for integrating complex sensory and neural functions and the initiation and coordination of voluntary activity in the body. [4]

For many years CP was known as Little’s disease because of William John Little, who was the first person to describe CP, in 1862. He described paralysis and spasticity of CP to be caused by damage to the brain in infants. [5]

The symptoms of CP can differ in type and severity between individuals, depending on which part of the brain that has been injured. The symptoms may also

change in a person over time even though the disorder is non-progressive. When a child grows up, some of the symptoms can become more or less evident.

In Sweden, about 200 children are diagnosed with Cerebral Palsy every year. [6] The overall prevalence of CP worldwide is 2-2.5 per 1000 live births and despite improved survival of at-risk preterm infants the prevalence of the disorder has remained constant [7][8]. The first clinical signs of CP can usually be observed in the early months of life but the diagnosis is often determined when the child is 2 to 4 years old [2] [3] [5].

### **2.1.1 Causes**

CP is caused by abnormalities inside a developing brain or when the brain gets damaged. The damages disrupt the brain's ability to control the movements of the body or maintain posture and balance. The damage can occur before, during or shortly after birth. Congenital cerebral palsy is the most common type of CP and means that the child is born with the disorder. A small number of children have acquired cerebral palsy, which means the damage occurred after birth. In those cases, potential causes of infections, head injury or problems with blood flow to the brain. However, many times the cause of CP is unknown. [3] [9]

### **2.1.2 Characteristics and symptoms**

The Surveillance of Cerebral Palsy in Europe network (SCPE) released a classification in 2000 that is used worldwide. According to this classification, CP can be classified into unilateral spastic, bilateral spastic, dyskinetic, ataxic and non-classifiable CP, see figure 1. The classifications are based on clinical signs where unilateral means that only one side of the body is involved while bilateral indicates that both sides of the body are involved. Spastic CP is the most common type of CP and is characterized by an increased tension in the muscles and a difficulty in controlling movement. Characteristics for dyskinetic CP is that the tone is varying, meaning that the child's movements are involuntary. Ataxic CP indicates that the child can have troubles with their balance and the coordination of movements. [9][10]

People with CP often have symptoms such as stiffness in some of their muscles, while being weaker in other muscles. The medical term for decreased muscle tone is hypotonia and it can make a person appear relaxed or "floppy". Hypertonia is the medical term for increased muscle tone and can make the person seem stiff or even rigid. [2] [3]



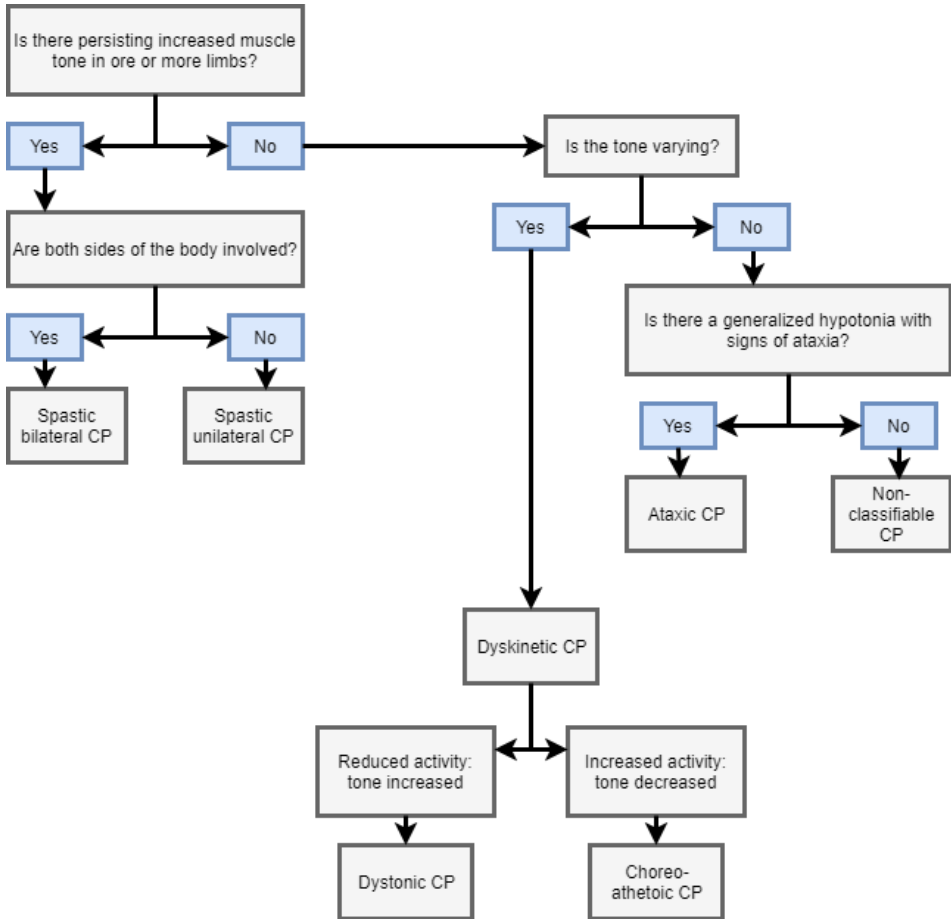


Figure 1: Subtype classification of Cerebral Palsy according to the SCPE network [10].

The imbalance between the muscles can lead to contractures, which is equivalent to a permanent shortening of the muscle and stiffness of the joints. In the hip joints there is a high risk that the contractures can cause dislocation of the hip (also called luxation of the hip). If there is an imbalance between the muscles around the spine, it can cause an abnormal curvature of the spine, called scoliosis. [6]

When a muscle is spastic, the stretch reflex increases and intensifies when the body part moves faster. This can lead to motor dysfunction and postural deficits, which limit the activity of the child, cause discomfort, may lead to contractures, skeletal torsion deformities and hip displacement. [5]

The main symptom in children with cerebral palsy is restricted motor function. The Gross Motor Function Classification System (GMFCS) is often used to describe the gross motor function in children with CP. It focuses on sitting, transfers and mobility and is based on five levels according to the self-initiated movement of the child. The different GMFCS levels can be observed in figure 2. [5]

A high GMFCS level is one of several parameters that is a well-known risk factor for hip luxation. For example, it has been shown that the risk for hip dislocation is 0% at GMFCS level 1 while it is 64% at GMFCS level 5. Other parameters that pose a risk for hip dislocation are young age, Windswept hip deformity (WS) and a high migration percentage (MP). While WS is a deformity in which one hip is in adduction and internal rotation, and the contralateral hip is in abduction and external rotation, MP is a radiographic measurement that describes the degree of lateral displacement of the femoral head. Treating WS is challenging and the condition has a negative impact on a child's ability to stand, sit and even lie down. Furthermore, WS is negatively affected by gravity. One-third of all children living with CP, at GMFCS levels 3-5, are affected by the condition. [5]

## GMFCS E & R between 6<sup>th</sup> and 12<sup>th</sup> birthday: Descriptors and illustrations

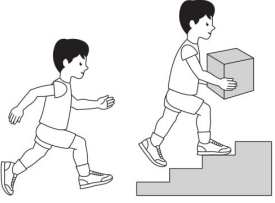
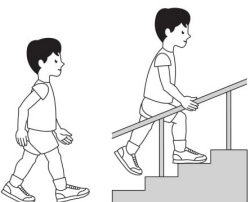
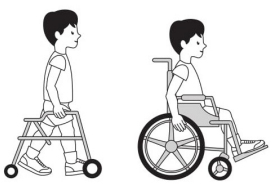
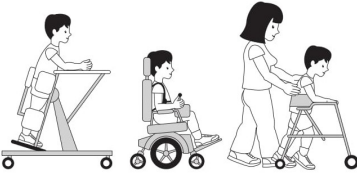
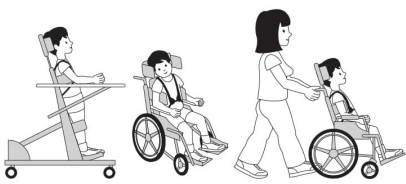
	<p><b>GMFCS Level I</b></p> <p>Children walk at home, school, outdoors and in the community. They can climb stairs without the use of a railing. Children perform gross motor skills such as running and jumping, but speed, balance and coordination are limited.</p>
	<p><b>GMFCS Level II</b></p> <p>Children walk in most settings and climb stairs holding onto a railing. They may experience difficulty walking long distances and balancing on uneven terrain, inclines, in crowded areas or confined spaces. Children may walk with physical assistance, a hand-held mobility device or used wheeled mobility over long distances. Children have only minimal ability to perform gross motor skills such as running and jumping.</p>
	<p><b>GMFCS Level III</b></p> <p>Children walk using a hand-held mobility device in most indoor settings. They may climb stairs holding onto a railing with supervision or assistance. Children use wheeled mobility when traveling long distances and may self-propel for shorter distances.</p>
	<p><b>GMFCS Level IV</b></p> <p>Children use methods of mobility that require physical assistance or powered mobility in most settings. They may walk for short distances at home with physical assistance or use powered mobility or a body support walker when positioned. At school, outdoors and in the community children are transported in a manual wheelchair or use powered mobility.</p>
	<p><b>GMFCS Level V</b></p> <p>Children are transported in a manual wheelchair in all settings. Children are limited in their ability to maintain antigravity head and trunk postures and control leg and arm movements.</p>

Figure 2: The five different levels of gross motor function according to the GM-FCS [5].

### **2.1.3 CPUP**

CPUP is a follow-up program for people living with cerebral palsy ([www.cpup.se](http://www.cpup.se)). The program started out as a collaboration between the departments for children orthopaedics and habilitation in Region Skåne, in 1994, after health care professionals had realized that many children with CP developed luxation of the hip joint, severe muscle contractures, joint stiffness and other symptoms. In CPUP, investigation of physiological and cognitive function is standardized and investigated continuously. Such continuous and standardized follow-ups allow early detection of physiological deterioration and create the conditions for providing preventive treatment in time. Today, CPUP is a national quality register and in summary its purpose is to create the best possible quality of life for people with CP, to increase the knowledge about CP and to improve the collaboration of management and habilitation of individuals with CP between different professions. [6]

### **2.1.4 Clinical examination and treatment**

Clinical examination of a child with CP in the CPUP program, is performed during visits to the hospital 1-2 times a year, depending on the GMFCS level. During this clinical examination the physiotherapist measures the range of motions of several joints, and examines the spine when the child is in a standing or in a sitting upright position. The child then bends forward and the degree of scoliosis can be classified. The hips are examined with the help of X-ray and with the subject laying on his or hers back. [5]

There are several different methods of treatment for decreasing the tension in the muscles and preventing contractures and dislocation of the hip. However, it's important that the necessary steps are initiated in an early stage. [5][6]

Preventive treatments include physical therapy, botox injected in spastic muscles, braces, orthosis and baclofen. Botox injections works by blocking the chemical signal between nerves and muscles that makes the muscles contract and tighten, and thereby reducing spasticity [11]. Baclofen, which is a drug, is another treatment that has a relieving effect on spasticity [12]. Operative treatments are sometimes used, such as soft-tissue release and skeletal surgery [5]. Soft-tissue release include tenotomies, in which the tendon is elongated surgically to relieve it from severe contractures [2].

## 2.2 The knee joint

The knee is a synovial joint, which is characterized by the presence of a fluid-filled joint cavity with cartilage covering the articulating bones and ligaments supporting the joint [13]. There are six different types of synovial joints. The knee is classified as a hinge joint, which is the most common type of synovial joint, in which the convex end of one bone is connected to the concave end of the adjacent bone. In a hinge joint, flexing and extending motions are allowed along only a single axis. Hence, such joints are uniaxial joints. [14]

However, the knee joint is a less typical form of hinge joint because it allows minor rotational and lateral movements. The degree of these movements depend on the position of the limb. [15]

### 2.2.1 Bones and muscles around the knee joint

The knee joint consists of three bones: the tibia, the femur and the patella. An illustration of the anatomy of the knee can be observed in figure 3. Two major muscle groups control the movements of the knee joint: the quadriceps muscles and the hamstring muscles.

The first-mentioned muscle group contains four muscles (vastus lateralis, vastus intermedius, vastus medialis and rectus femoris) which are located on the anterior side of the thigh. By contracting and shortening these muscles, the leg is extended. The hamstring muscles on the other hand, flex the knee when activated. This muscle group is situated on the posterior of the thigh and knee joint and consists of 3 muscles (biceps femoris, semimembranosus and semitendinosus). An illustration of the knee joint and the muscles that work during flexion and extension can be observed in figure 4. [15]

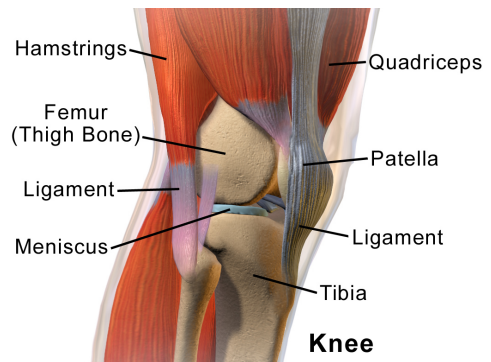


Figure 3: The anatomy of the knee [16].

### 2.2.2 Flexion and extension of the knee joint

The rotation between the tibia and the femur bone has a “screw-home” mechanism occurring between full knee extension (0 degrees) and 20 degrees of knee flexion.

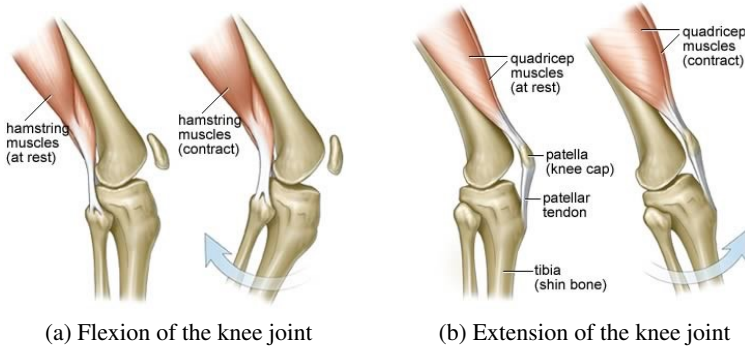


Figure 4: The knee joint and the muscles surrounding it [17].

In this last phase of knee extension, the tibia rotates externally onto the femur resulting in the cruciate ligaments being tightened which locks the knee joint into a stable position that inhibits rotational movements between the two bones. [18]

Motion takes place in all three planes in the knee joint. However, the range of motion is greatest in the sagittal plane as full extension of the knee generally is 3 degrees of extension while full flexion of the knee is up to 155 degrees of flexion [19]. Because of this, the angle of interest for continuous measurements in this project is the knee flexion angle. When measuring the maximal flexion angle and extension angle, it is important to distinguish between active motion and passive motion because the latter is usually 5-10 degrees larger. The reason to this is that passive motion is performed by the measurer applying a force to reach the extremes of flexion and extension while active motion is when the subjects themselves apply muscle forces to reach the extremes of motion.

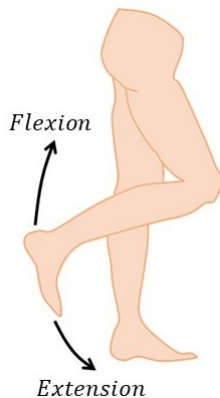


Figure 5: Flexion and extension of the knee.

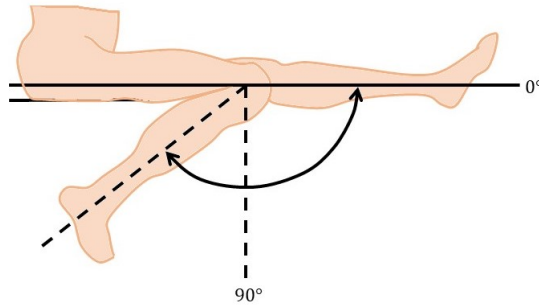


Figure 6: The range of motion of the knee.

Illustrations of the flexion and extension of the knee and the range of motion of the knee can be observed in figure 5 and 6. [19]

Two larger studies of range of joint motion in different age and sex groups have been performed. One of the studies measured active range of motion (AROM) in normal children aged 3 to 9 years while the other measured passive range of motion (PROM) in normal children aged 2 to 8 years [20][21]. The maximal knee flexion angle from these studies are presented in table 2.1.

PROM (2-8 years)		AROM (3-9 years)	
Female	Male	Female	Male
152.6	147.8	144	145

Table 2.1: The maximal knee flexion angle for PROM [20] and AROM [21].

When developing the measurement device, the AROM values from table 2.1 were used as guidelines for setting the minimal angle range requirement for the device.

### 2.2.3 Gait and flexion deformity of the knee

The extent of contractures, joint stiffness and bone deformities vary in patients with CP and because of this, the prevalence of gait deviations varies. Impairments causing gait deformities vary in severity and it is common with asymmetric impairments between the two legs. Even though there is a wide range of gait deformities, some are more common than others. One of the most common gait deformities in patients with cerebral palsy is drop-foot gait during which active ankle dorsiflexion is inhibited because of muscle hypotonia. Dorsiflexion occurs during the swing phase and because of this, patients with drop-foot tend to experience foot dragging and tripping [22]. Another common gait abnormality is

inadequate knee flexion during the swing phase, causing a reduced foot and toe clearance, meaning that the foot's height from the ground is reduced. Such reduction in knee flexion is identified as stiff-knee gait and patients often experience, just as people with drop-foot gait, foot dragging and tripping during walking [23].

Flexion deformity, or flexion contractures, of the knee refers to the inability to fully straighten the knee. One of the most common problems in children with CP is contracture of the hamstring muscles, which can progress to fixed knee flexion contractures. Patients with knee flexion contractures are often walking with a bent-knee gait which increases the strain on the knee joint and the muscles surrounding the knee. This can lead to the person developing a crouched gait pattern which can be painful and reduce ability to walk. Treatments include physiotherapy, knee orthotics and, in more severe cases, surgical treatment. [24][25]

The complexity of gait deformities depends largely on the fact that some kinematic deviations may come secondary to other problems or as compensation for another gait deviation. Moreover, impairments are rarely isolated; therefore, gait deviations are often the results of combinations of impairments. Considering the fact that patients with CP present numerous combinations of impairments, managing gait deviations is complex. Many different types of treatments exist, with physiotherapy being the most common, to maintain, improve, preserve or restore a patient's range of motion, muscle strength, balance and coordination. Another common treatment for managing gait deviations is applying orthoses. A so called ankle-foot orthosis for example, is frequently used for treating a gait deviation where the person is walking on his/her toes, which many people with Cerebral Palsy tend to do. [26]

## **2.3 Sensors and software**

In this project two different measurement techniques were tested in order to fulfill the main objective. These techniques were based on using an inertial measurement unit (IMU) and a potentiometer, respectively. Their functions and characteristics are described in the following sections along with the software program that were used to test and develop the device.

### **2.3.1 Inertial measurement unit**

An inertial measurement unit (IMU) is a combination of measuring devices used for calculating and tracking orientation and movement of a body. The unit usually contains one accelerometer, gyroscope and magnetometer per axis. In this project,



three-axis IMUs are used and every axis has one each of the three different measuring devices. [27]

In the IMU, the accelerometer detects linear acceleration while rotational rate and the magnetic field surrounding the sensor are detected by the gyroscope and the magnetometer, respectively. These different measurements can then be used for describing orientation by calculating Euler angles, which represent a sequence of three elementary rotations around the axes of a coordinate system. [27]

Euler's theorem states that "an arbitrary rotation may be described by only three parameters". The orientation of a body can be achieved by creating three rotations about the axes of a coordinate system. The Euler angles are the three angles that describe the orientation of the rigid body with respect to a fixed coordinate system. These rotations can be extrinsic, which means that the rotations are about the axes of the original coordinate system that remain fix, or intrinsic, which means the body changes its orientation after each element rotation. [28]

There are different types of sequences for the Euler angles but the one used in this project are called Tait-Bryan angles. Tait-Bryan is commonly applied when using IMUs and is, simply explained, used for calculating rotations around the x-axis (roll), y-axis (pitch) and z-axis (heading). Roll, pitch and heading can be calculated in different ways. [27] [29]

In this project the following equations have been applied initially [29]:

$$Roll = arctan\left(\frac{Accel_y}{Accel_y^2 + Accel_z^2}\right) \quad (1)$$

$$Pitch = arctan\left(\frac{Accel_x}{Accel_x^2 + Accel_z^2}\right) \quad (2)$$

The equations will provide the pitch and roll values for the accelerometer data. The accelerometers measure both acceleration due to the movement of the sensor and due to the gravity of the earth. [29]

The gyroscope provides data for the angular velocity, which is linear to the rate of rotation. The gyroscope is quick to respond to changes in the angular velocity and is not affected by earth's gravity. To obtain the rotation from the gyroscope one can simply time-integrate the value:

$$\int_a^b f(x) = Gyro_{axis} * dt \quad (3)$$

where the specific gyro data is chosen depending on if the rotation is around the x- or y-axis, i.e. the roll or pitch angle. The calculated result drifts over time,

yielding unusable results. The reason for the drift is that when integrating the angular velocity, a small inherent (mechanical/hardware) offset becomes dominant. [29][30]

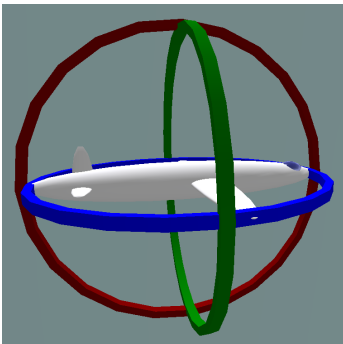
In order to measure the heading, data from the magnetometer is needed. The equation for calculating the heading is [31]:

$$\text{Heading} = \arctan\left(\frac{Mag_x}{Mag_y}\right) \quad (4)$$

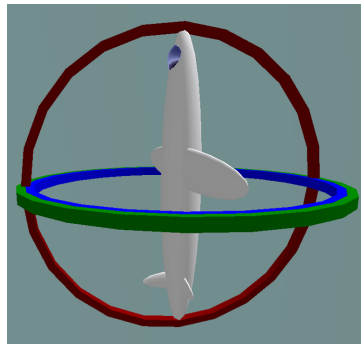
These equations, 2 to 4, provide the angles in radians.

### 2.3.2 Gimbal lock

A problem with Euler angles is that a phenomenon called Gimbal lock occurs. The Gimbal lock happens in the gyroscope, which contains gimbals. A gimbal is a pivoted support that allows rotation of an object around a single axis. When Gimbal lock happens, the axes of two of the three gimbals are parallel to each other, causing the system to rotate in two-dimensions instead of three, see figure 7. One way to avoid Gimbal lock is to apply quaternions instead of using the Euler angles. [32]



(a) No Gimbal lock: all three gimbals are independent [33].



(b) Gimbal lock: two out of the three gimbals are in the same plane [34].

Figure 7: A visual explanation of Gimbal lock.

### 2.3.3 Quaternions

Quaternions are an extension of the complex numbers and consists of four numbers: a scalar and a three-component vector;  $q = (w, xi, yj, zk)$ , where  $w, x, y,$  and  $z$  are all real numbers and  $i, j,$  and  $k$  are quaternion units. The real numbers

w, x, y, and z are normally in the range between -1 and 1. The absolute values of them added together is equal to 1. These real numbers make it possible to reorient vectors in a single rotation. [35]

In 3D rotations, which is how they are applied in this project, quaternions are defined as

$$q = [\cos \frac{1}{2}\theta, \sin \frac{1}{2}\theta v] \quad (5)$$

where  $v$  is the axis which the vector is rotated about by an angle of  $\theta$ . However, as can be observed in equation 5, only half of the angle  $\theta$  is used in the equation [36].

### 2.3.4 Potentiometer

A potentiometer consists of three pins, a resistive track and a sliding contact that can rotate around the resistive track. When used as a voltage divider, the two outer pins are connected to ground (GND) and to the positive voltage supply (+Vcc), respectively, while the middle pin gives the voltage output. Whenever the sliding contact is rotated, the current's path through the track is changed. In other words, the path becomes longer or shorter when the sliding contact is moved, resulting in a change in the resistance of the potentiometer. A picture of a carbon track potentiometer can be observed in figure 8 and the sliding function can be observed in figure 9. [37][38]



Figure 8: A carbon track potentiometer [39].

The circuit diagram for when the potentiometer is used as a voltage divider can be observed in figure 10. When the potentiometer is connected as a voltage divider, its function is to turn a large voltage into a smaller one and the output voltage can be calculated from Ohm's Law:

$$V_{out} = V_{cc} * \frac{R_2}{R_1 + R_2} \quad (6)$$

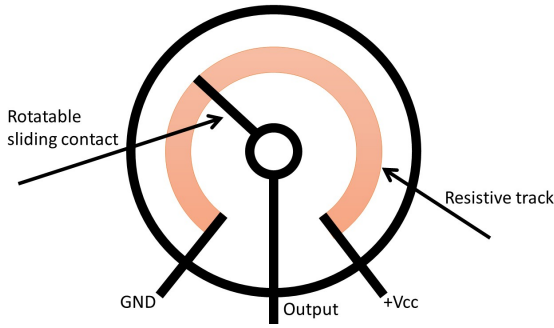


Figure 9: The sliding function of a potentiometer.

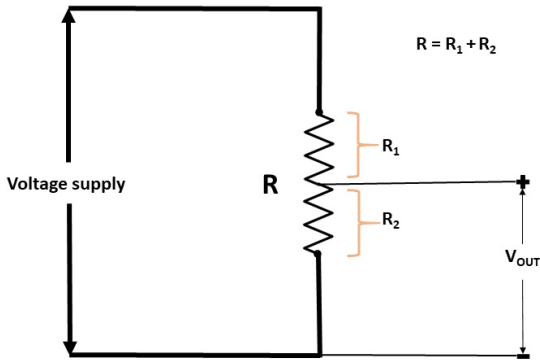


Figure 10: The circuit diagram of a potentiometer.

While there are different types of relationships between the resistance of the potentiometer and the position of the sliding contact, the two most common ones are linear and logarithmic potentiometers. In this project, a linear potentiometer was used. [37][38]

### 2.3.5 Arduino

Arduino is an open-source hardware and software company. They design and manufacture microcontrollers and kits for building digital devices and objects that can interact, sense and control other physical objects. The microcontrollers are programmed using a language that is similar to the languages C and C++. Microcontrollers and software from Arduino has been used in this project as a tool to create and develop the measurement device. [40]

## **2.4 Product development process and software development**

When developing the measurement device, code for data collection and processing along with a wearable equipment had to be developed. A general process, explained below, for product development was implemented for the entire project and more specifically, iterative and incremental software development was applied for generating all project code.

A major part in this project was testing different sensors and with that, writing task-specific code of varying complexity. For collecting and processing data from the sensors, code in Arduino, Matlab and Excel was created and improved through both iterative and incremental development.

### **2.4.1 Iterative development**

An iterative design method performs a cyclic design process in which the steps of prototyping, testing, analyzing and refining a product or process are repeated. It is always the most recent iteration of a design that is tested and changes and refinements are performed based on the testing results. This cyclic process aims at improving the quality and functionality of a design. [41]

### **2.4.2 Incremental development**

An incremental build model is a method of software development, where a product is designed, implemented and tested by adding a little more to the product each time. Hence, the development of the product is incremental. When all of the product requirements are satisfied, the product is defined as finished. The incremental build model utilizes a combination of the so called waterfall model and iterative prototyping. [41]

### **2.4.3 General product development**

The product development process contains six phases: planning, concept development, system-level design, testing and refinement, and product ramp-up. For this project, only the phases of planning and concept development are of interest because of the fact the other phases concern, and are more applicable in, manufacturing. Applied to this project, the planning phase consists of specifying the

goals, key assumptions and constraints for the product. The concept development phase is explained more thoroughly in the following subsection. [42]

### **2.4.4 Concept development**

A concept describes the function, features, required specifications and design of a product [42]. The concept development process contains many different steps in which the requirements of the product are identified and various product concepts are generated and evaluated. In the end, one or several concepts are further developed and tested. Moreover, this phase usually contains benchmarking which is an analysis of relevant, similar and/or competitive products. Benchmarking has been performed in this project to gather inspiration for developing an ergonomic, user-friendly and lightweight wearable measuring device. In this project, the concept development was sectioned into six subsequent steps [42]:

1. Identifying and understanding customer requirements
2. Establishing target specifications
3. Concept generation
4. Concept selection
5. Concept testing
6. Setting final specifications

### **2.4.5 Identifying customer needs**

The process of identifying customer needs involves gathering raw data from interviews, focus groups and/or by observing the product in use. In interviews, the interviewer discusses needs with a single users, while in focus groups, the interviewer take the role of a moderator and facilitates a discussion with a group of users. The raw data is then analyzed and needs are described in terms of what the product has to do and/or be like. Identified needs are then to be categorized into primary and secondary need statements, where the primary are the most general needs while the secondary express needs in more detail. The relative importance of the need statements is established by performing further user surveys and/or by performing an importance assessment based on previous experience with users. [42]

In this project, customer requirements were obtained through an interview with Gunnar Hägglund, an orthopaedist with years of experience concerning children

with Cerebral Palsy, and through a literature study and benchmarking. The results were then used for establishing different target specifications and for generating and implementing a concept. The definition of target specifications and a process for concept generation are presented below.

#### **2.4.6 Establishing target specification**

These specifications are expressed in technical terms and are based on the user requirements. An example of a target specification is what type of unit the device, developed in this project, need to have as output and what margin of error is allowed. Target specifications enables a more precise and detailed description of a product necessary function and form. [42]

#### **2.4.7 Concept generation**

Concept generation is used to find creative ways to solve the specific problem. The method can, according to Ulrich and Eppinger [42], be divided into five steps:

1. Clarify the problem. Understand the problem and decompose it into smaller subproblems.
2. Search externally. Gather information from lead users, experts, patents, published literature, and related products.
3. Search internally. Use individual and group methods to retrieve and adapt the knowledge of the team.
4. Explore systematically. Use classification trees and combination tables to organize the thinking of the team and to synthesize solution fragments.
5. Reflect on the solutions and the process. Identify opportunities for improvement in subsequent iterations or future projects.

#### **2.4.8 Concept selection**

During the concept selection the generated concepts are analyzed to find the best concept. [42]

### **2.4.9 Concept testing**

During this step the selected concept is tested to verify that the best concept is chosen and that it meets the customer requirements. [42]

### **2.4.10 Setting final specifications**

During this final step the target specifications are compared to the selected concept. [42]

## **2.5 Previous research**

In 1988, Tardieu et al [43] performed a study on children with CP where they investigated the period of time per 24 hours during which the child's muscles had been stretched and for how long the muscles must be stretched to prevent contractures. During several months Tardieu et al performed both passive measurements and 24-hour measurements on children with CP, under conditions that did not interfere with their usual activities or therapy. The range of passive soleus muscle (calf muscle) stretch was calculated from the following measurements. Angle 1 was the angle at which a minimal torque, i.e. a fully extended knee, was recorded, while angle 2 was the maximal torque, i.e. when the knee is fully bent. The difference between these two (angle 1 - angle 2) gave the range of motion for passive soleus muscle stretch. These angles were measured before, during, and after the 24-hour period of interest.

The measurements were made using a potentiometer that was connected to a device which recorded the output during a 24-hour period. The 24-hour measurements provided information on the range of ankle motion used by the child over the 24-hour period. It also measured the amount of time for which the ankle joint was at each angle interval and when the soleus muscle was stretched beyond a minimal threshold. [43]

The study from Tardieu et al [43] was the main inspiration and a springboard for this project. However, the focus of Tardieu's study was mainly on the ankle joints and the calf muscles, while the main objective in this project was to measure the angle motion of the knee joint. The aim was to develop the idea and measurement technique used by Tardieu et al by implementing a more ergonomic, user-friendly and wireless solution, using modern technology. The methods of measuring knee contractures in children with CP are limited and the most common way of assessing the patients are by measuring different range of motions during visits to the



hospital. If the physician or physiotherapist were able to receive collected long-term data and evaluate the patient's active range of motion, it might be possible to detect and treat contractures at an earlier stage and customize the treatment for every child. [23][24]



## 3 | Initial information gathering

The process and results from the initial information gathering are presented below.

### 3.1 Initial information gathering

A literature study within the fields of measuring devices, Cerebral Palsy and gait analysis was initially performed to gain a deeper understanding of the problem and to find material for the background chapter of this report. The literature study was initiated using the Snowball method [44][45] on the review article ‘A review of e-textiles in neurological rehabilitation: How close are we?’ by Ruth McLaren et al.

References from McLaren et al [46], Tardieu et al [43] and Tognetti et al [47] were used to find suitable studies for the project and key words to use for a literature search using LubSearch, the search engine for finding library resources at Lund University [48]. Literature searches were then performed continuously as the project progressed. Suitable articles were found when screening previous articles for citations.

The clinical supervisor of the master thesis provided up-to-date dissertations on the subject of cerebral palsy. These were used as references and as a way to find more research on the subject.

In the beginning of this project, the function and use of IMUs were investigated. The initial literature search focused on finding research where IMUs were used for measuring body movement and tracking of joint rotation. During the initial literature search, articles that were not relevant for the project were excluded. No exclusion criteria by publication date were made due to the initial lack of articles on the subject. Only articles in English and Swedish were included.

### 3.1.1 Results from initial information gathering

11 articles were identified when reading the initial three articles that were determined useful for the project. The search words that were identified in the articles can be observed in table 3.1 and were used for the literature search in LubSearch. 98 articles were identified by using the search words. After remov-

Cerebral palsy	Joint motion
Children	Active range of motion
Gait analysis	Range of motion
Measurement	Joint range of motion
Goniometer	Ankle
Inertial measurement unit	Knee
Wearable sensor	Norms
Spasticity	Normal

Table 3.1: The search words used in the initial literature search

ing duplicates and screening titles and abstracts, 14 articles remained for full-text screening. More articles were added continuously during the project due to the iterative method of working. The initial review article, McLaren et al [46], identified two areas of research focus; motion sensing, and the measurement of, or stimulation of, muscle activity. The article aimed to determine if there was any substantial evidence to support the use of e-textiles in the rehabilitation of people with neurological conditions. The conclusion was that there was a lack of high quality clinical evidence and also, a lack of practicality for clinical application.

McLaren et al identified articles on the subject of measuring joints using different types of wearable sensors [47][49][50][51][52][53][54]. Articles on gait analysis using wearable sensors was also identified [55][56][57]. Yang et al [56] and Sung et al [57] focused mainly on prototype designing and did not assess the reliability of their calculations against another method of gait analysis.

The main conclusion that could be drawn from the initial literature search using the search terms, was that there was a lack of research in the area of CP combined with long term measurement devices. Most of the wearable measurement devices lacked practicality and had not been tested clinically. Articles that studied the use of goniometers were identified from the search terms [58][59][60]. Van den Noort [59] used inertial sensors as reference system to evaluate the use of goniometry. Articles investigating the use of inertial measurement units for joint measurement were also identified [61][62][63][64][65][66]. The identified articles that studied the possibility on implementing inertial measurements to measure joint movement

was limited and the procedures were complicated.



## 4 | Initial specification of requirements

The initial literature search and the interview with Gunnar Hägglund resulted in an early specification of requirements for the measurement technique. The specification of requirements was used as a guideline during the development process and are presented below:

- Be able to measure the angle of knee flexion. To measure the angle correctly, the potentiometer needs to be placed in the center of rotation.
- Be able to measure correctly during 24 hours without any drift of the measurements and a maximum of 2-3 degree error.
- Be able to collect and save data during 24 hours.
- Easy processing of data to find the duration the knee is positioned in certain angles.

The measurement technique is to be used on children with CP that has a GMFCS level of 1 to 3. This is because these children are mobile enough to move around and the right physiotherapy can help them to lower the GMFCS level or prevent them from progressing to a higher level.





# 5 | Development of IMU measurement device

This chapter will present the development process of using IMU sensors to create a measurement device along with the results obtained during the process.

The process of solving the problem of continuously measuring joint angle and developing a prototype was both incremental and iterative. When developing the software for the prototype, it was designed and tested by initially solving a more simple version of the problem and gradually adding a little more complexity to it. Hence, applying an incremental build model to the development process. During this incremental design approach it became evident that the project members did not have enough understanding nor time to learn the more complex side of IMUs. Due to these facts, it was not possible to configure the IMU-sensors to correctly measure joint angles. The IMU-sensors also lacked certain capabilities in order to be used for accurately measuring joint angles. Therefore, a different approach using a potentiometer, presented in chapter 6-7, was tested.

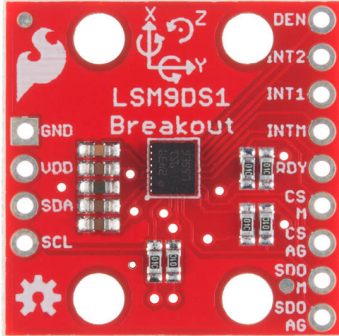
An iterative design process, in which prototyping, testing, analyzing and refining the prototype are repeated, was applied to both the software and the wearable device development.

## 5.1 Initial implementation of the IMU sensors

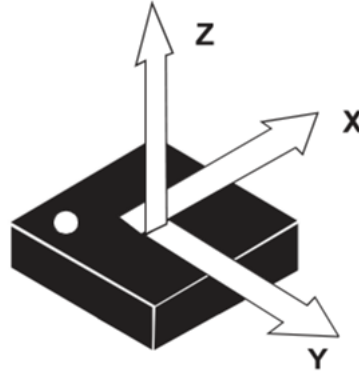
The initial approach of this project was to implement IMU sensors and measure the angle between the sensors. The supervisor provided the project with the following material:

- 1 Breadboard
- 1 Arduino Nano

- 2 SparkFun 9DoF IMU Breakout - LSM9DS1
- Wires to connect the components to each other
- 1 USB cable to connect the Arduino Nano to the computer



(a) The pinouts of the IMU.



(b) The axes of the IMU.

Figure 11: The SparkFun 9DoF IMU Breakout.

The IMU sensor and its pinouts can be observed figure 11a, along with the axes of the IMU, see figure 11b. Pin headers were soldered onto the IMU to be able to connect it easily to the breadboard. Using the Sparkfun Hookup guide [27], specific for the LSM9DS1 IMUs used in this project, a single IMU was connected to the Arduino Nano. The Arduino Nano was then connected to the computer using the USB-cable and the pre-written code for the IMU was downloaded and implemented in the Arduino platform [67]. The standard code continuously printed values for the accelerometer, gyroscope and magnetometer. These values changed as the breadboard was rotated around the IMUs x-, y- and z-axis.

The initial focus was on the pitch and roll angles, which represented the rotation around the IMU's y- and x-axis. They were calculated using data from the accelerometer in the IMU, using equations 2 and 1. Arduino code that calculated the pitch and roll angles for a single IMU was developed and implemented.

The next step was to connect a second IMU to the prototype and calculate the pitch and roll angles for both sensors. The set-up of the Arduino Nano and the two sensors can be observed in figure 12.

When connecting the second IMU it was discovered that it had the same address as the first IMU. This meant that the location of data from the two IMUs had the same address, a unique number, assigned to them. Hence, the Arduino could not

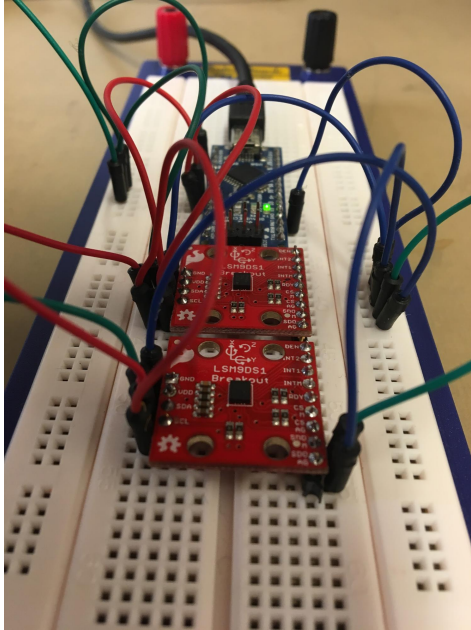


Figure 12: Arduino Nano connected to two IMUs.

distinguish the two IMUs from one another and it was only possible to obtain data from the IMU defined first in the software code. This was solved by connecting the SDO-AG-channel on the second IMU to Ground on the Arduino.

When printing the pitch and roll values for the two sensors, it was noted that the sensors did not measure the same values even though they were positioned identically. Their different offsets from zero were measured and the calculated values were adjusted accordingly. However, the pitch and roll values were drifting and were very sensitive to movements. Because of this, a contribution from the gyroscope data, see equation 3, was added and a complementary filter was implemented. The filter consisted of different weight functions for the contribution from the accelerometer data and the gyroscope data. The reason for implementing this approach was that the gyroscope provides more accurate short term data while the accelerometer provides more accurate long term data. The equations used are presented below:

$$angle = weight_1 * (angle + gyroPitch) + weight_2 * accelPitch \quad (7)$$

$$weight_1 + weight_2 = 1 \quad (8)$$

When fitting the complementary filter, three different combinations of weight functions were evaluated on the following criteria:

- Time for adjusting offset
- Stability during movement
- Angle continuity during stationary positions

When moving the sensors, both slow and fast movements were tested. The slow movements consisted of rotating the sensors around their y-axis, with approximately a speed of 18 degrees per second. The fast movements consisted of rotating the sensors around the same axis, but with approximately a speed of 180 degrees per second.

Once again the offset for the sensors were calculated by placing them in a stationary position. However the surface was not entirely flat so the calculation was not considered completely accurate. This offset calibration made the signal close to zero when in a flat and stationary position. When keeping the signal stationary at other angles it slowly drifted back to zero. To try to remove the drift a more advanced calibration based on the nonlinear least square method was considered [68]. This was not successful and it was difficult to measure the accuracy of the different angles as the sensors were attached to the breadboard.

### 5.1.1 Results from the initial implementation of the IMU sensors

The different weight functions and the time for the adjusted offset to stabilize, i.e. for the filter to stabilize, can be observed in table 5.1. Even though the weight function with  $weight_1$  set to 0.96 and  $weight_2$  set to 0.04 required the longest time, 15 000 ms, to stabilize, it was selected for further development. The reason for this was that it had the most stable reaction during movements. It also provided the most continuous angles when the sensors were in stationary positions.

$Weight_1$ (gyroscope)	$Weight_2$ (accelerometer)	Time for adjusting offset (ms)
0.96	0.04	15 000
0.97	0.03	10 000
0.98	0.02	10 000

Table 5.1: The different values that were tested for the weight functions and the time necessary for full offset adjustment.

Even when using the complimentary filter, signals from both sensors slowly drifted towards zero and the implementation of the nonlinear least square method was unsuccessful. However, the signal drifted with such a low rate that the project continued with developing a measuring method by using the approach with the complimentary filter.

## 5.2 Initial angle measurement using IMU sensors

The sensors were soldered onto individual, smaller boards and connected to the Arduino using long cables. This was to enable measurements of the angle between the two sensors.

The sensors were then attached to a special made protractor which made it possible to measure and observe the real angle while collecting data from the IMUs, see figure 13.

The angle between the sensors was calculated by subtracting the pitch value (calculated using the complimentary filter) of one sensor from the other. This made it possible to measure angles between -180 and +180 degrees, which fit the requirements for the project.

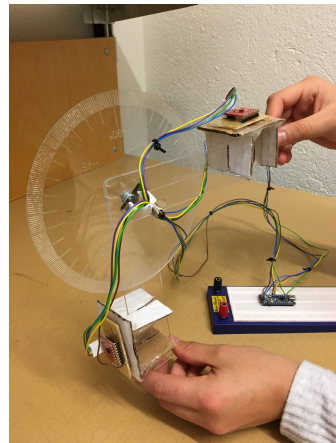


Figure 13: Two IMUs attached to a protractor.

The software Coolterm [69] was used to capture data when measuring the pitch value at different angles (0, 45, 90, 135). During these measurements the roll value of the device, and hence the roll of both IMUs, was close to zero, meaning that the IMUs were only rotated around the global Y-axis and not around the global X-axis. For visualization of IMU axes in relation to global axes and planes, see figure 14. Data was collected for 1 minute and the standard deviation was calculated using Matlab, by applying the function  $std(A)$  to the last 500 values in each matrix.

When tilting the device in different roll angles, meaning that the IMUs' local y-axes were not parallel with the global Y-axis, the pitch data from the sensors drifted majorly and became inaccurate. The result of this was that when the device was tilted to the side, around the global X-axis, it was no longer possible to use the pitch angle to calculate the angle of rotation around the y-axis. One approach

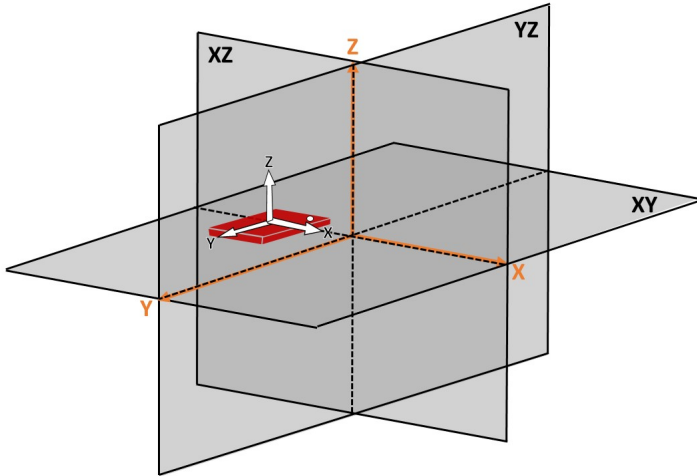


Figure 14: IMU axes in relation to global axes and planes.

that was tested was combining pitch and heading by evaluating the roll angle. The idea was to read the roll angle and weigh the pitch and heading together in the following way:

- When roll equals 0 degrees, use pitch angle.
- When roll equals 90 degrees, use heading angle.
- When roll is somewhere in between 0 and 90 degrees, combine pitch and heading angle by applying different weight functions.

When attempting to implement the magnetometer by calculating the heading, using equation 4, it was discovered that the values were too sensitive and unreliable for long term use.

Due to the inaccuracy when measuring with the sensors in a tilted position and the uncertainty with the magnetometer, a new approach was attempted using a different kind of IMU sensor.

### 5.2.1 Results from the initial angle measurement using IMU sensors

Data was collected from the two sensors for different angles and using the weight function with the following values for weight:  $weight_1 = 0.96$  and  $weight_2 = 0.04$ . The angle was measured when the sensors were in an upright position (when the roll angle equals approximately 0 degrees) and the standard deviation of the data was calculated in Matlab. The standard deviations for the different angles

can be observed in table 5.2.

Pitch Angle (degrees)	Error, standard deviation
180-0	-0.641
180-45	-1.012
180-90	-0.213
180-135	-0.292

Table 5.2: The standard deviations for the different angles.

When the roll angle was approximately 0 degrees, it was observed that the device calculated the angles with a small standard deviation. However, when the device was tilted (Rotated around the global X-axis) the values from the sensors drifted and the sensor could no longer measure the pitch angle. The reason for the system not being able to accurately calculate the pitch angle is due to the pitch angle being partly calculated from the accelerometer data, which is affected by gravity. For example, for movements when the IMUs y-axis is parallel to the global Y-axis, see figure 14, i.e. movements in the global XZ-plane, the contribution from gravity in both the x- and the z-direction will vary. Because of this variation in gravity, the two IMUs' pitch values will differ from each other, except if both IMUs either have pitch equal zero or 90 degrees, and the angle between them can be estimated. Whenever the IMUs y-axes are parallel to the global Z-axis, i.e. movements in the global XY-plane, the contribution from gravity will be close to constant in all three axes and hence, different angles will be calculated to the same value. In other words, whenever the sensors' local XY-planes are parallel to the global XZ-plane, the output will be of a constant value even if there is a change in the angle between the sensors.

To summarize, the closer the roll angle is to 90 degrees, the more equal is the contribution from gravity on the two IMUs. The result of this being that the device calculates an increasingly inaccurate and more and more constant angle between the two IMUs even if their local xy-planes are rotated differently from each other. To solve this problem, the magnetometer was implemented but without success.

Another problem that occurred with the IMUs was that whenever the device was subjected to shock, for example shaking the device, the measurements became very unstable and it took a long time for the system to stabilize. This is an aspect that also contributed to trying a different sensor.

### 5.3 Implementing IMU sensors with absolute orientation

A new IMU-sensor was used, Adafruit's IMU sensor with 9-DOF - BNO055 [70]. This sensor had an built-in processor where it supposedly calculated the absolute orientation, quaternions and the Euler Angles from the data obtained from measurements.

A similar model to the previous prototype was created with the new sensors. A new Arduino software program was written where different methods were used to calculate the angle and the results were compared.

Initially, the same approach as with the Sparkfun sensors was tested. However, this time the Euler angles could be obtained directly from the sensor and hence, no Euler equations needed to be implemented in the code. There were three different ways to obtain the angles:

- Using the Euler function and receive pitch, roll and heading in a vector.
- Using the function *getEvent()* and obtain three orientation coordinates (angles)  $-x$ ,  $y$  and  $z$ .
- Derive the quaternions and then convert them to angles using the function *toEuler()*.

These three ways to find the angle between the sensors turned out to deliver almost identical results with similar issues, meaning that the system was able to accurately measure angles only when the sensors local y-axes are parallel with the global Y-axis.

#### 5.3.1 Implementing a weight function using pitch, roll and heading

Measurements when the roll angle was between 0-90 degrees were, just as with the sensors from Sparkfun, inaccurate. Because of this, and the fact that the magnetometer values from the new IMU showed more stable and promising values, a similar weight function to the one tested with the IMUs from Sparkfun was implemented. To clarify, only pitch needed to be used for zero degrees roll tilt, see figure 15, while only heading needed to be used for 90 degrees roll tilt, see figure 16. In figure 17 on the other hand, a combination of heading and pitch angles needed to be calculated. Many different weighting functions needed to be applied depending on the two sensors' positions in space.

When using the heading angles it was discovered that the two sensors mirrored each other in opposite directions. This was solved by making the sensors in phase



with each other by adding 180 degrees to one of them.

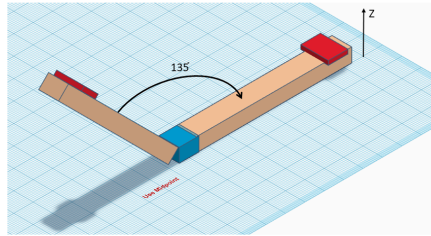


Figure 15: 135 degrees between sensors and no tilt.

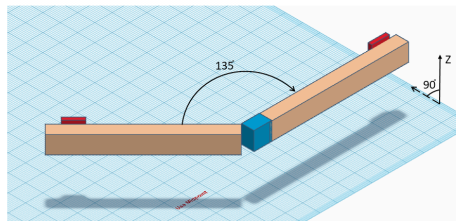


Figure 16: 135 degrees between sensors and 90 degrees tilt.

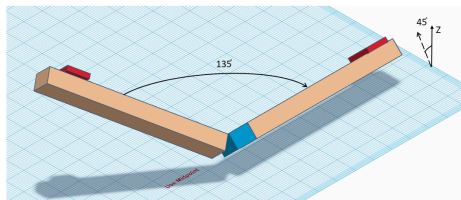


Figure 17: 135 degrees between sensors and 45 degrees tilt.

Another problem that occurred was that the three orientation angles had different ranges. The heading had a range that was from 0 to 360 while the pitch angle had a range from -90 to 90 degrees. The result of this was that when the pitch angle was used for calculating the angle between the IMUs, an angle of 135 degrees would be displayed as only 45 degrees, i.e. the angle would decrease after 90 degrees. Because of this, the pitch values needed to be adjusted to be able to compare them to the heading values. This was solved by calculating the dot product for the two IMUs' quaternions and solving for the angle between the quaternions.

### 5.3.2 Using quaternions to find the angle

The BNO055 IMU from Adafruit calculated quaternions and Euler angles in a global system, meaning that the orientation of two IMUs could be related to each other. To calculate the angle between the two IMUs, an approach based on the dot product formula was implemented. By using the two sets of quaternions, which are four-dimensional vectors,  $Q_1$  and  $Q_2$ , the dot product formula in equation 9, 10 and 11, could be used to calculate the angle between the IMUs.

$$Q_1 \cdot Q_2 = |Q_1||Q_2| \cos \theta \quad (9)$$

$$\cos \theta = \frac{Q_1 \cdot Q_2}{|Q_1||Q_2|} \quad (10)$$

$$\theta = \arccos \frac{Q_1 \cdot Q_2}{|Q_1||Q_2|} \quad (11)$$

The quaternions for each sensor orientation could also be derived directly from the sensors. By calculating the dot product for the two quaternions and solving for the dot product angle, an angle estimate was obtained. However, only approximately half of the true angle value was calculated through the dot product method. The reason for this is that quaternions by definition use half the angle  $\theta$ , i.e.  $\theta/2$ , see equation 5. Therefore, the angle from the dot product was multiplied by 2. By doing this, any error became twice as large. To visualize the problem, the quaternion dot product for the experimental setup was calculated for different angles, while rotating the setup in different directions, see figure 18.

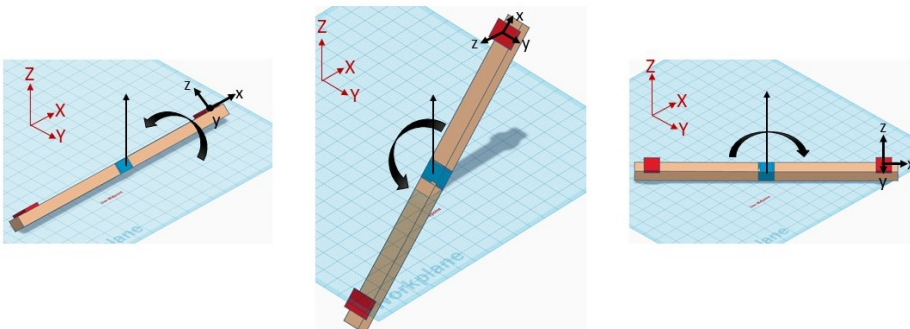


Figure 18: Rotations around the global X-, Y- and Z-axis.

### 5.3.3 Results from implementing IMU sensors with absolute orientation

The new sensors from Adafruit were implemented in the same way as the ones from Sparkfun. The same results as with the Sparkfun sensor were obtained when measuring the angle when in an upright position, i.e. for movements in the global XZ-plane. The Euler angles could be derived directly from the sensors without using the equations as previous.

#### 5.3.3.1 Results from implementing a weight function using pitch, roll and heading

Obtaining the pitch angle from the sensors was easy and it was possible to obtain an accurate angle when the sensors were in an upright position. When the device was tilted, i.e. the roll angle increased from zero to 90 degrees and movements occurred in the global XY-plane, the pitch angle decreased to zero. In the 90 degrees tilted position, the heading angle was accurate and therefore used instead. Whenever the roll angle was in between 0 and 90 degrees, i.e. the sensors were in a plane that was tilted in relation to the global XZ-plane, neither the pitch angle nor the heading angle were accurate and they were very unstable. An attempt of implementing weighting methods to enable accurate angle measurement was performed. However, the relationship between the two angles varied immensely depending on position in relation to each other, the earth's magnetic field and the contribution from gravity. Finding the different weights and the situations for which they should be implemented became very complex and time-consuming. Because of this, the approach with using quaternions for calculating the dot product angle was explored and developed instead.

#### 5.3.3.2 Results from using quaternions to find the angle

The mean value and standard deviation, for three different angles, from the dot product application were calculated through Matlab with the resulting values presented in table 5.3.

True angle (deg)	$2 \times \text{Mean}$ (deg)	Std (deg)	Measurements	Sample time
0	5.5378	2.5750	1590	2 min 45 s
45	46.0772	4.7245	1493	2 min 35 s
90	90.8738	2.3741	1416	2 min 27 s

Table 5.3: Dot product angle for different fixed angles and positioning of IMUs.

A problem with using the dot product occurred whenever the two IMUs did not have the same tilt on their XY-plane, see figure 19. Since the dot product is dependent on all the vectors' dimensions, a setup as in figure 19 would result in two different local body systems, i.e. the coordinate systems would not coincide. Even though the two IMUs would refer to the same global system, performing dot product on two separate local system would result in calculating an angle that does not correspond to the true flexion/extension angle. Instead it would show an angle where the limbs are twisted in relation to each other.

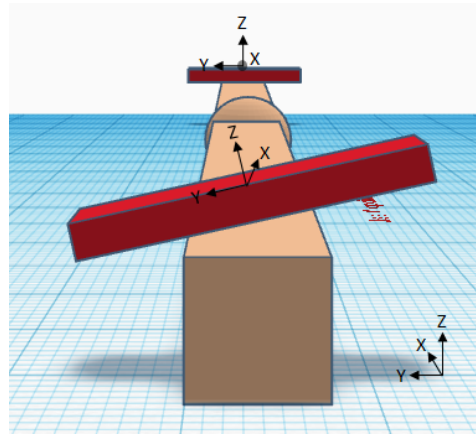


Figure 19: Visualization of two IMUs with different tilt on their xy-plane.

A positive aspect with the approach of using quaternions is that stable angles can be calculated when the set-up is moved in space. That is, if arranging the two sensors in a specific way and then rotating and moving this set-up, the output angle would be stable. However, as previously concluded, only half of the true angle value was calculated which results in any error becoming twice as large when doubling the calculated angle. In conditions when the two sensors have close to the same tilt on their xy-plane, the angle error vary approximately from 5 to 10 degrees, (approximated from table 5.3), which is a rather large error. Whenever imperfect tilt conditions occur between the two sensors, the calculated angle differs much from the actual angle. Hence, the system calculations become unrepresentative for the actual angle. A third problem observed with quaternions is that they are affected by magnetic fields. Moving the sensors close to, for example, smart phones and computer displays resulted in greatly unstable output values.

Lastly, a fourth obstacle was encountered. When performing various tests with the IMUs, the output could randomly flip to and stabilize at a completely different value. This happened repeatedly in different intervals throughout all tests.

Troubleshooting was performed but without success. This obstacle was the main reason the project changed focus, and combined with the other factors affecting the stability and the reliability of the measurement method, another approach was implemented. The new approach was based on using a potentiometer, just as Tardieu et al, for measuring joint angle motion, or more specifically the knee flexion angle.



# 6 | Development of potentiometer measurement device

After experiencing problems with inadequate and incorrect angle measurements with the IMU approach, a new procedure using a more hands-on technical solution was conducted. A carbon track potentiometer was used to implement a method for obtaining the joint angle.

This chapter includes the developing process regarding implementation of a potentiometer to create the measurement device, followed by the development of the wearable measurement device that will result in the final prototype.

## 6.1 Initial implementation of potentiometer

A linear potentiometer was attached to a goniometer with a pointer, see figure 20, to be able to relate the analog read from the potentiometer to a certain angle. The analog read from the potentiometer was in the range of 0 to an A/D value of 1023 and the pointer was able to rotate 270 degrees.

The potentiometer was connected to the Arduino Nano and data was collected and analyzed using the programs CoolTerm and Matlab. The data was collected for 10 seconds at every 10th degree on the goniometer, i.e. from 0 degrees to 270 degrees.

Mean values of the collected data were calculated and used to perform a curve fitting in Matlab, with the A/D values acting as x-values and the angles acting as y-values. As expected, a linear curve, and equation 12, was obtained.

$$y_{angle} = k * x_{A/Dvalue} + m \quad (12)$$

The k and m values for the plotted linear curve was used in the Arduino code to convert the potentiometer analog output to degrees. A validation of the linear

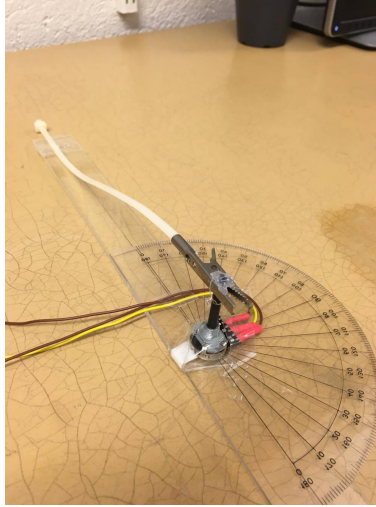


Figure 20: The potentiometer attached to a goniometer.

equation was performed by comparing the calculated angle with the angle from the goniometer.

One of the main problems with the potentiometer and the analog output/angle-relationship was identified; the potentiometer was not completely linear in the beginning. The output was unstable between zero and 40 degrees. This was considered a purely mechanical issue that depended on the potentiometer used in this project and could not be resolved. To bypass this unstable region of the potentiometer, the adjustable resistance in the potentiometer was set in such way that the analog output gave an A/D value of 908 at the zero-degree mark of the goniometer.

### 6.1.1 Results from initial implementation of potentiometer

The collected data (in A/D value) for the potentiometer showed that the potentiometer increased linearly between 40 and 240 degrees. Using the collected data, a curve was fitted between 40 and 240 degrees on the goniometer.

A plot of the A/D value and the measured angle can be observed in figure 21. It shows linearity between 40-240 degrees. The data in this range was used to calculate the curve fitting in Matlab. The angle range for the device was determined to be sufficient because of the fact that active range of knee joint motion is approximately 145 degrees in children aged 3 to 9 years [21], see table 2.1.

The linear fit from the data can be observed in figure 22 and gave the following



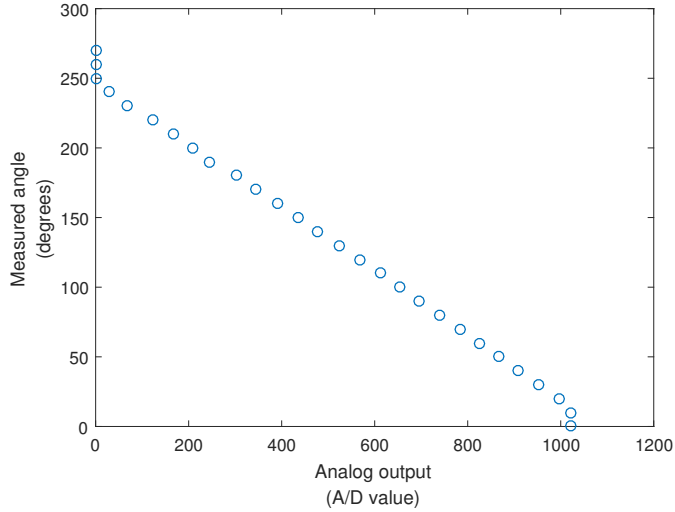


Figure 21: Measured angle and collected A/D value from initial implementation.

equation:

$$Degrees = (-0.23) * A/D\ value + 209 \tag{13}$$

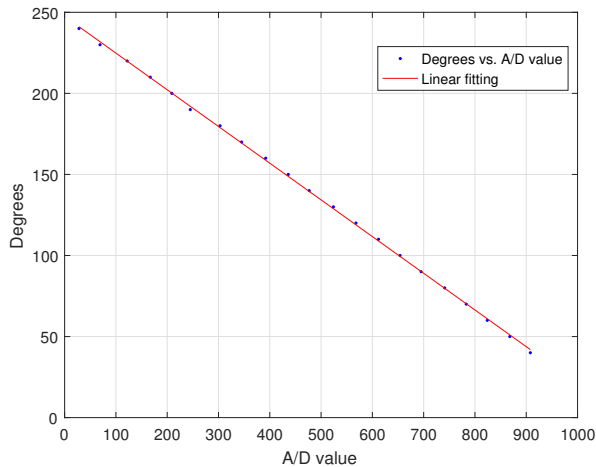


Figure 22: The linear fit from the data measured with the potentiometer.

The goodness of the fit was evaluated by calculating the R-squared and the Root Mean Squared Error (RMSE) through the Matlab operation called Curve Fitting. A short explanation of R-squared is that it provides a statistical measure of how close the data is to the fitted regression line [71]. R-squared values lie between 0

and 1, with the value of 1 implying a model that perfectly predicts values in the target field. RMSE on the other hand, is the standard deviation of all the prediction errors (residuals) and it has the same unit as the dependent variable which in this case is degrees [72].

R-squared was calculated to 0.9997 which indicated that the linear fit was good. The calculated RMSE, 1.115 degrees, too implied that the linear fit was satisfactory since the RMSE was small enough compared to the normalized data range of 0-200 degrees (40-240 degrees).

After applying the equation from the linear fit on the output in the Arduino code, data was collected from the potentiometer in the same way as previously. Data was collected every 10th angle, for the entire potentiometer range of 270 degrees. From that data collection, data for the range 40-240 degrees was normalized and can be observed in table 6.1. The RMSE for the angle estimation for the normalized data in the table was calculated to 1.4310 degrees.

## 6.2 Developing a wireless system

2 LiPo batteries, an Adafruit MicroSD card breakout board, a micro SD card and a LiPoly backpack was used to make the device wireless. The SD breakout board and a LiPoly backpack were soldered onto a new microprocessor, Adafruit Pro Trinket. This was due to the old Arduino Nano stopped working and no similar microprocessor was available. This was not a problem as the Trinket was very similar to the Arduino Nano.

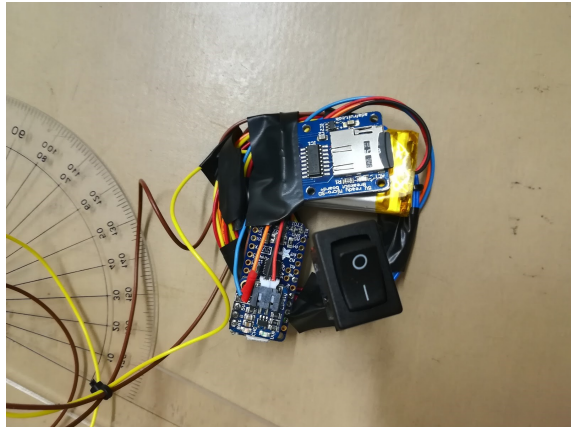


Figure 23: The wireless system of the device.

The LiPoly backpack made it possible to connect a LiPo battery to the device. A LiPo battery, or a lithium-ion polymer battery, is a lightweight, rechargeable battery that is being used in applications such as cellphones and tablets [73].

An on/off switch was also connected to the LiPoly backpack, which made it possible to turn the device on and off. The complete wireless system can be observed

Angle G (measured from goniometer)	Angle P (measured from potentiometer)	A/D value
0	0	908
10	9	868
20	19	824
30	29	783
40	39	741
50	49	695
60	59	654
70	68	612
80	78	568
90	88	524
100	99	477
110	109	436
120	119	392
130	130	345
140	139	303
150	150	257
160	161	209
170	171	167
180	181	123
190	193	69
200	203	28

Table 6.1: The normalized data from the potentiometer along with the angle measured from the goniometer.

in figure 23.

The Trinket was then connected to the potentiometer and data was collected on the SD card in the form of a text file. The data could then be analyzed in Matlab.

It was possible to collect the data accurately from the potentiometer but not possible to implement a real time clock into the device. This made it more difficult to visualize the data in regard to the time. The time stamp of the collected data was interesting to obtain because it made it possible to relate the flexion angle to the time of the day, and hence to certain activities. To solve this the Arduino function *Millis()* was used in the Arduino code. *Millis()* returns the number of milliseconds since the Arduino board began running the current program [74]. The *Millis()*-time was then collected and split into hours and minutes and added to a starting time that was noted in the beginning of the data collection.

An issue that occurred with the new microprocessor, the Trinket, was that it did not have a serial port, i.e. the same possibility of monitoring the data in real time as the Arduino Nano. This made it difficult to test the accuracy of the device without needing to collect data on the SD card every time. This was solved by connecting a FTDI cable to the FTDI port on the Trinket. This enabled serial connection and made it possible to monitor the data in real time. However, the solution was not ideal as six different wires from the microprocessor needed to be connected to the FTDI cable every time there was a need to monitor the data.

The Arduino code was uploaded to the microprocessor using the FTDI cable and the program was initiated. The SD breakout board indicated when the measurements started with a led light flashing on the board. The led light would flash in the same rate as the measurements were collected. The wireless prototype was then tested by collecting data on the SD card and analyzing the data in Excel. A simple program was created in Excel to simplify the data analysis and visualization of the collected data for the potential user.

### **6.3 Developing a wearable prototype**

After developing and testing the potentiometer measuring device on the experimental setup, i.e. the goniometer, and observing promising and satisfactory results, the project proceeded into the next phase where a wearable prototype was developed.

The development process was iterative and consisted of identifying user requirements, establishing target specifications and concept generation. A measuring device, such as the one developed in this project, can be considered as having three different users - the physician, the parents and the patient. A set of requirements were identified after having discussed the needs of patients and physicians with Professor Gunnar Hägglund and after having read multiple articles on developments of similar devices. The target specifications were established based on the identified requirements.

Finally, concept generation was performed by benchmarking similar products, such as knee orthoses, and via generating ideas through brainstorming and brain-drawing. The last mentioned is a type of visual brainstorming in which participants sketch their ideas to possible solutions. Examples of the sketches can be observed in figure 24 and 25.

The sketches varied in detail and complexity, some described a more general solution while others described detailed solutions for a specific design problem, for example how to secure the potentiometer to the stationary and the mobile splints.

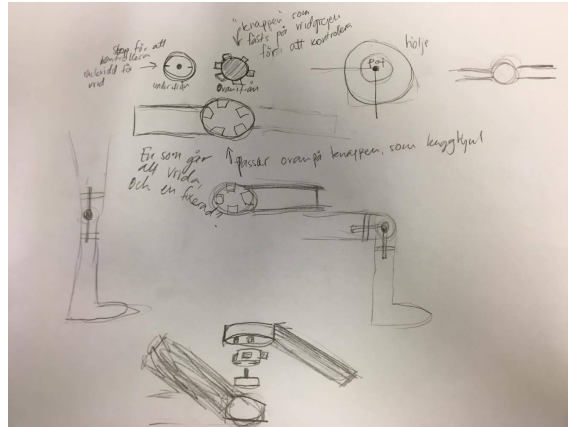


Figure 24: One of the sketches that was created during the brainstorming and braindrawing sessions.

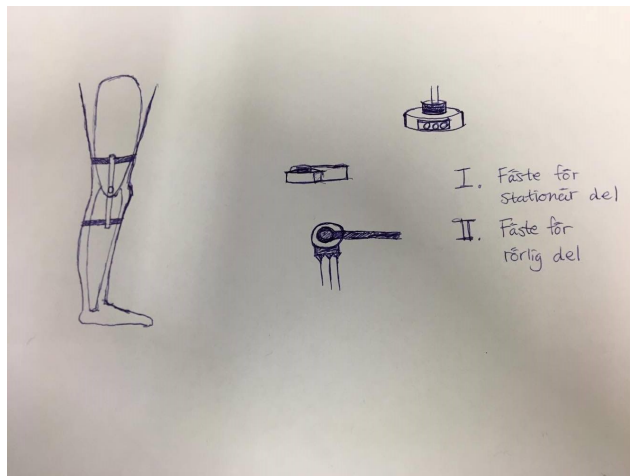


Figure 25: A more detailed sketch of the selected concept.

After discussing and evaluating the different ideas, a simple concept design was selected for further development.

Using the concept design, two plastic splints were cut out and attached to the potentiometer. The design was tested on one project member using Velcro and tape to secure it.

A simple concept design of a wearable prototype was selected for further development and can be observed in figure 26.

It was decided that the wearable device should include the following aspects:

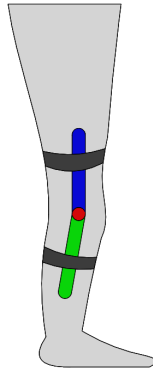


Figure 26: The initial concept design of a wearable prototype.

- A potentiometer placed on the lateral side of the rotation center of the knee joint.
- Two plastic splints attached to the potentiometer, one to its stationary part and one to its moving part.
- Two sets of Velcro-tape, one for fastening the stationary splint and one for fastening the mobile splint.
- Space for placement of microprocessor, battery and sd card holder.

Using the concept design the project proceeded with creating a more detailed target specification. The important points and specifications can be observed in the target specification in section 6.3.1.

### 6.3.1 Target specification

This target specification for the measurement device was created from the simple concept design. The first part considers the technical specifications and are followed by the ergonomic specifications and the including components that need to fit on the leg along with the measurement device. Finally the last part declares the specification of requirements for the device. Some of the specifications below are the initial requirements that were mentioned in chapter 4 of this report.

The main users of the device were identified as three different types of users: the child who wears the device, the parent who puts it on the child and turns it on and off, and the physician or physiotherapist who analyses the collected data.

### **6.3.1.1 Technical specifications**

- Be able to measure the angle of knee flexion. To measure the angle correctly, the potentiometer needs to be placed in the center of rotation.
- Be able to measure correctly during 24 hours without any drift of the measurements and a maximum of 2-3 degree error.
- Be able to collect and save data during 24 hours.
- Easy processing of data to find the duration the knee is positioned in certain angles.
- A light brace with a joint in the middle where the potentiometer is attached.

### **6.3.1.2 Ergonomic specifications**

- Attached to knee with soft knee pad and Velcro tape to minimize affecting movement of the knee
- Comfortable
- Suitable for children
- Easy to put on and take off

### **6.3.1.3 Components that needs to fit on the leg**

In addition to the potentiometer there are several external components that need to be placed on the leg without interfering with the measurements or the movement of the person wearing it. The components that needed to be considered are as follows:

- 1 LiPo battery
- 1 micro SD breakout board + SD card
- 1 microprocessor of the type Adafruit Pro Trinket
- Pro Trinket Lilon/LiPoly Backpack
- 1 on/off button

The components were measured and cut out of paper to enable an easier way to brainstorm how they should be placed above the knee. In figure 27 one can

observe one way of placing the components. To protect the wires and the components the idea was to place them inside a plastic compartment.

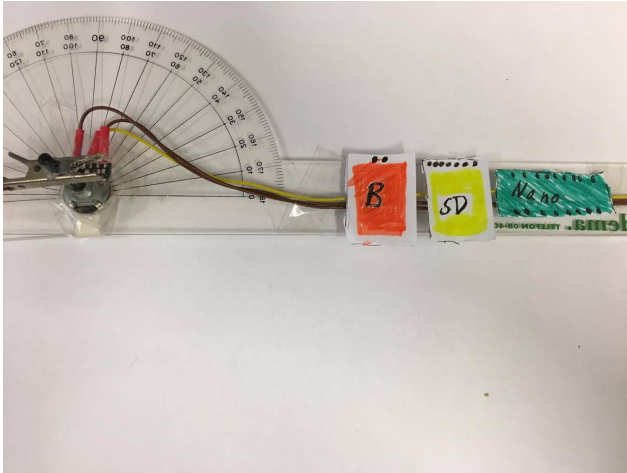


Figure 27: One of the ideas on how to place the components on the device.

### 6.3.1.4 Specification of requirements

Using the specifications in the sections above, a detailed specification of requirements were created for the next step in the development process. The requirements can be observed in the list below:

- One plastic splint, A, with a hole where the bottom part of the potentiometer fits. The splint should be approximately 20 cm long and the diameter of the hole should be 16 mm.
- One plastic splint, B, with a hole for the rotating rod. The splint should be approximately 15 cm long and the diameter of the hole should be 4 mm.
- Both splints should be 3 cm wide and have rounded edges.
- Splint A is to be attached to the rotating rod so when it moves, the rod rotates.
- Splint B is to be glued onto the bottom side of a button that is fixated onto the rotating rod.
- The potentiometer needs to be attached to rotation center.



## 6.4 The first wearable prototype

The plastic splints were cut out of acrylic glass and attached to the potentiometer according to the specification of requirements. The external components were bundled together and attached above the knee while the potentiometer was placed in the rotational center of the knee, with splint A pointing up towards the thigh and splint B pointing in the opposite direction. The prototype positioned on the leg can be observed in figure 28.



Figure 28: The first wearable prototype.

### 6.4.1 Measurements from the first wearable prototype

Measurements were collected during 50 minutes while one of the project members was wearing the prototype. The measured data was saved on the SD card and later processed in Matlab. The collected data was plotted with the time and can be observed in figure 29. The plot shows a few outliers that are higher than 200 degrees which is anatomically impossible. The reason for this data was considered to be due to the device being sensitive to chock and some of the wires being lose.

The battery life of the prototype was also tested by keeping the device turned on during several days to collect data. The results from the testing showed that

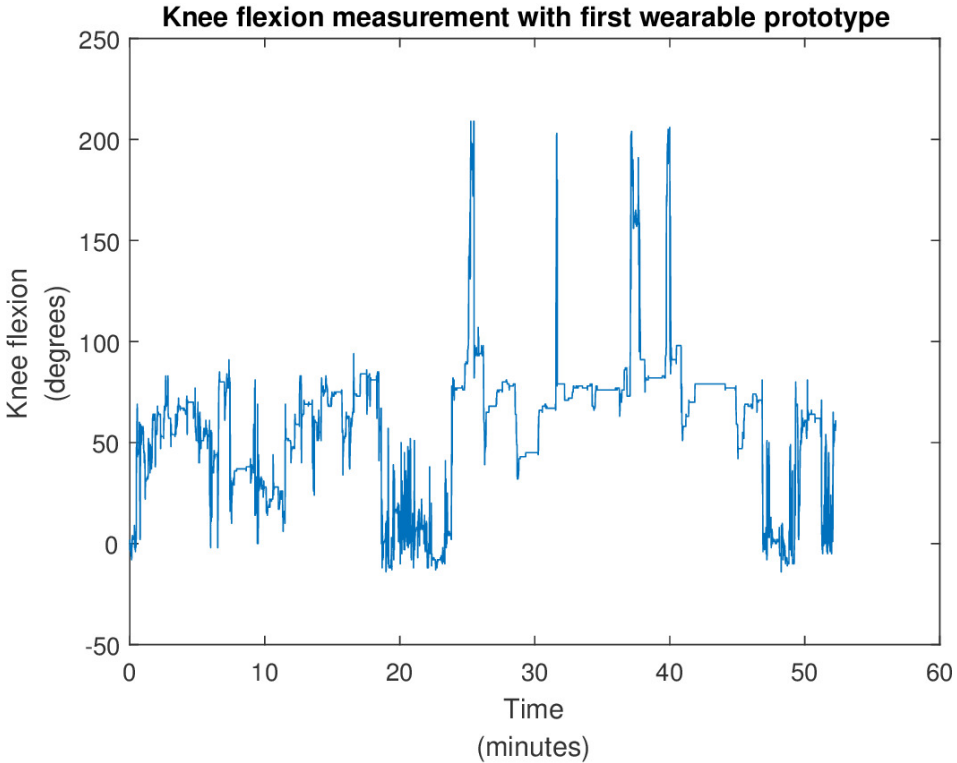


Figure 29: Measurements from using the first wearable prototype.

the battery lasted for about 30 hours, when it was not fully charged from the beginning, and that data had been collected during the whole time. This showed that the device satisfied its requirements for battery life and ability to collect data during a longer time period.

### 6.4.2 Further development of the first wearable prototype

After collecting data using the first wearable prototype, alterations were made to improve it. The wires that connected the potentiometer to the external components were changed to lighter, thinner and shorter wires. All of the external components were fitted into a plastic compartment, that can be observed in figure 30.

An issue that occurred during measurements with the first wearable prototype was that the plastic splints did not stay in place using the Velcro. Hence, a new solution was needed. A new approach was tested using a sock to fixate the device. The sock on its own was not enough to hold the device in place so it was combined with the Velcro strips. This can be observed in figure 31.

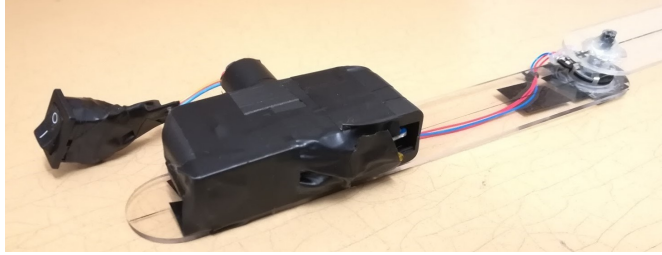


Figure 30: The external components fitted into a compartment.



Figure 31: An attempt to use a sock to fixate the device.

The solution with the sock and Velcro strips was considered to be deficient due to the sock not being resistant and holding the device in place. The sock was swapped for a knee pad where the device was attached with elastic web on the outside of the knee pad. The plastic splints were also shortened because they were considered unnecessary long.



## **7 | The final prototype**

After several iterations the final prototype was created. The development of the final prototype will be presented below, followed by a presentation of the collected and analyzed data from the final prototype.

### **7.1 Developing the final prototype**

The prototype with the knee pad was considered to be most suitable for further development. The device was fixated on the knee pad using elastic web. The compartment for the external components was fixated above the knee. This was later considered, by the project members, to be uncomfortable and resulted in attaching the compartment below the knee.

### **7.2 Results from the final prototype**

The final prototype can be observed in figure 32 and 33. The prototype consists of a knee pad with elastic ribbons sewn onto the lateral side, where the device is attached. This makes it possible to first put on the knee pad and then attach the device to the knee pad, without risking damaging the device. The compartment with the microprocessor, SD card and the other components is placed in the front, below the knee and on the inside of the knee pad.

The purpose of the device is to be able perform long-term measurements of range of motion of the knee in children with CP. As the children are being evaluated at a young age, it is likely that the parent will be the one who puts on the device and turns it on and off. Removing the SD card and loading the data onto the computer can either be done at home by the parent or by the physician or physiotherapist at the hospital. The battery lasts for over 30 hours which means that the child can wear the device for a longer period of time without having to charge the battery.



Figure 32: The final prototype using a knee pad.



Figure 33: The final prototype using a knee pad.

This can instead be done between two long term measurements, by the parent or at the hospital. While the battery is stored in a compartment that needs to

be opened in order to remove it, the SD card is accessible and can be removed without opening the compartment.

During the testing of the final prototype, data was collected during different types of physical exercise such as walks and squatting, and analyzed in Matlab to investigate if it was possible to distinguish the different types of exercise. Data was collected with a sample rate of 2 Hz (i.e. 2 samples/second). This low sample rate was selected because it was of interest to see how seldom data could be collected and still represent an accurate range of motion movement.

The collected data during a period of two hours can be observed in figure 34. One can clearly see in the figure that the test subject is walking, where the measured angle is smaller, in comparison to a larger flexion angle when seated, and the movement of the knee is increased.

An interesting observation is that the measured angle decreases during the outdoor walk. The first part of the outdoor walk was downhill while the second part of the walk had a slight incline. A study by Wen-Yi Chen and Ching-Shan Lin concluded that the larger the incline is, the smaller are the knee joint angles compared to during normal level walking [75]. At the same time, the study also showed that the larger the decline is, the larger is the knee flexion angle. Hence, with those results in mind, the reason for the angle decrease in figure 34 is likely due to the fact that the walk went from a downhill slope to an uphill slope.

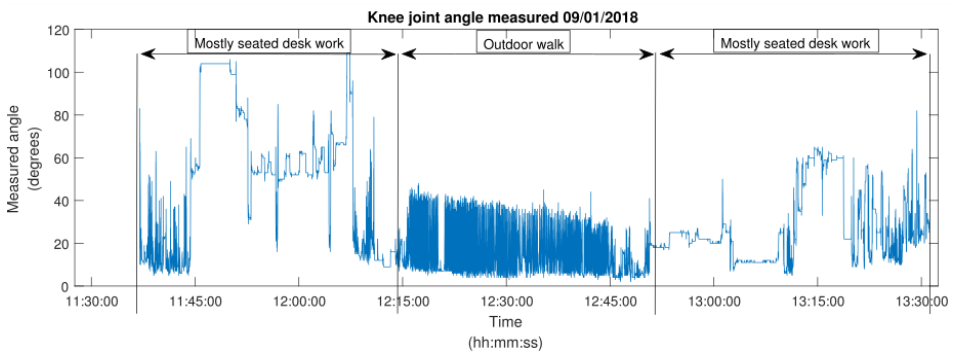


Figure 34: Collected data from the final prototype.

Even though the results in figure 34 look promising, the largest knee flexion angle recorded during the downhill walking is approximately 50 degrees. This is a much lower value than the reference peak value for gait during level walking, which is approximately 70 degrees [19]. The reason for not detecting angles corresponding to that, or even higher since downhill walking results in larger knee flexion, can either be that the sample rate of 2 Hz was too low for accurately recording knee flexion angles during walking or that the physical design of the prototype prevents

## The final prototype

full motion. It is not unlikely that the relatively low flexion angles are a result of both too low sample rate and too rigid prototype.

Due to one of the main target groups being physicians, a program for analyzing data was created in Excel. The SD card can then be inserted to a computer where the data can be loaded directly into the program in Excel, which can be observed in figure 35. This was to make it more accessible for the physician to collect and analyze the data when evaluating a patient.

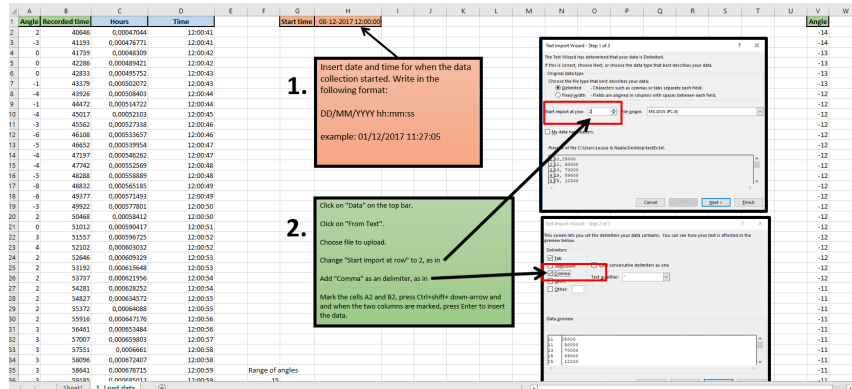


Figure 35: A screenshot from the program in Excel.

As aid for the physician or physiotherapist in the evaluation of a patient it would be interesting to find the angle distribution during the period of measurement. A histogram was created in Excel and can be observed in figure 36. When looking

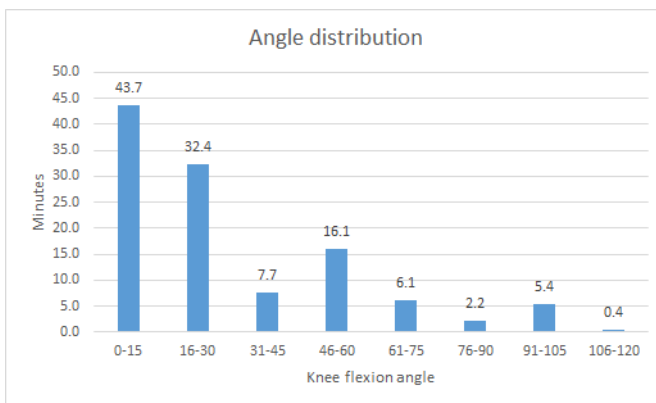


Figure 36: The distribution of angles in the collected data.

at the histogram one can see what angle range is the most frequent in the collected data. In this case the device has collected 43.7 minutes of data when the knee is



in 0-15 degrees of flexion. In Tardieu et al [43], the collected data was analyzed by creating a cumulative plot, which is a similar way of analyzing the data as the one chosen for this project. By sorting the angles in a histogram it is possible for the physician to detect significant movements of the knee that could indicate contractures.

Data from the two hour test, figure 34, was collected at a low sample rate, approximately 2 Hz. Such low sample rate could be accepted when seated or for instance during sleep, i.e. for rather long term stationary situations. For dynamic situations, such as gait, a higher sample rate is required in order to properly visualize the flexion-extension angle of the knee.

Since gait deformities are a common occurrence in people with Cerebral Palsy, it was of interest to see how well the final prototype could record a gait cycle. Therefore, another test was performed during gait with an extreme sample rate of approximately 100 Hz. Several gait cycles recorded from that test can be observed in figure 37. To further analyze the prototype's capability to accurately record and calculate knee flexion angle during gait, one gait cycle was compared to a reference gait cycle, see figure 38. As can be observed from the figure, the two plots have similar shape. Nevertheless, the two plots differ in several aspects. Firstly, the reference plot, figure 38b, starts at zero degrees while the neither the cycle in 38a nor none of the cycles in 37 starts at zero. Instead, these cycles start at around 7 to 10 degrees. Secondly, the first peak has a magnitude of approximately 18 degrees in 38a while 38b has less than 10 degrees in magnitude. Likewise, the second peak differs approximately 15 degrees between the reference plot and the one recorded by the prototype.

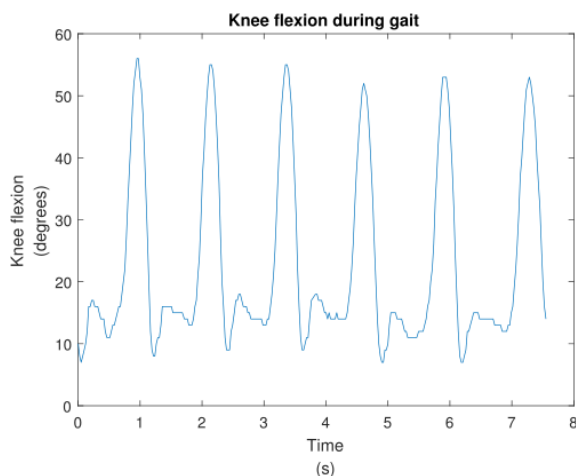
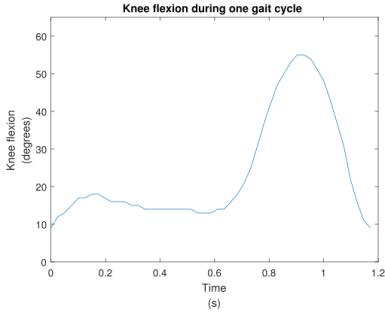
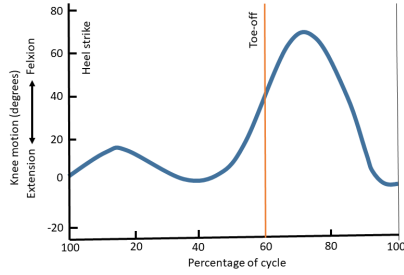


Figure 37: Several gait cycles from the collected data.



(a) A single gait cycle from the collected data.



(b) A single gait cycle adapted from [19].

Figure 38: A comparison between one measured gait cycle and a reference example.

A possible explanation to why the prototype has an offset of ten degrees is that when the subject had a straight leg, the two plastic splints on the prototype were not aligned but instead had a small angle between them. The reason for the second peak to be lower than the reference value can be that the prototype prevents the last degrees of movement.

To further evaluate the prototype, data was collected when the test person performed squats. The knee flexion during one squat can be observed in figure 39.

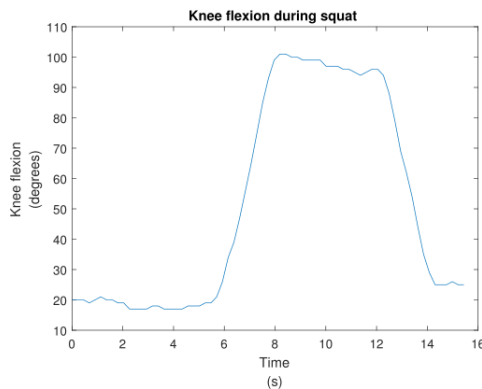
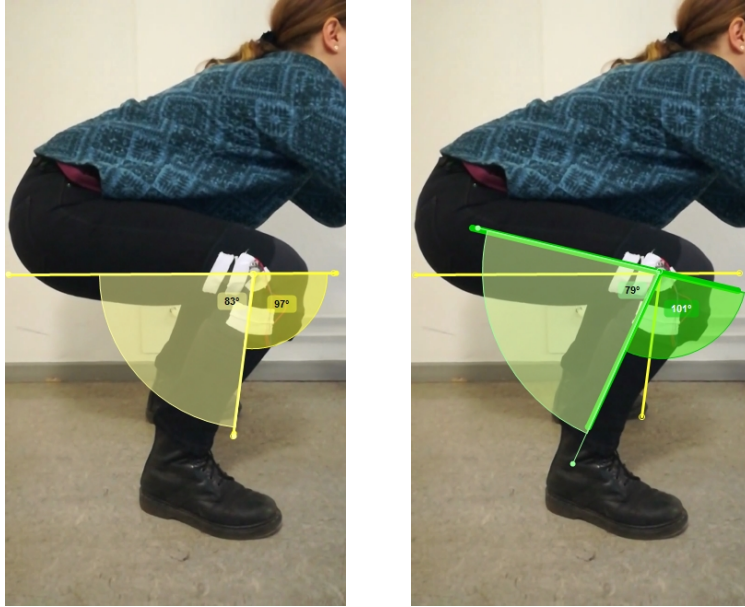


Figure 39: The knee flexion during one squat.

To be able to compare the data measured with the device, the squats were also filmed and analyzed using the software Kinovea [76], where it is possible to measure angles in recorded movies. Furthermore, the flexion angle during full squat was measured with a goniometer.



(a) The angle measured by the device visualized using the Kinovea software.

(b) The measured angle of the leg using the Kinovea software.

Figure 40: A picture of a squat using the Kinovea software.

Figure 40a displays the angle of 97 degrees measured by the prototype. The two lines with an angle of 83 degrees between them represent the positions and directions of the two splints. As visible, both splints deviate from the actual direction of the femur and tibia, which is visualized in figure 40b where 101 degrees represent the actual knee flexion angle. This deviation and the fact that it seems as the prototype restricts motion to some extent, during for example gait, suggest that the prototype is not flexible enough. Hence, the prototype can become more accurate and reliable by improving its adherence to the leg, thus preventing the prototype from twisting or revolving around the leg, and by improving its flexibility to flexion/extension movements.



# 8 | Discussion

This chapter discuss the work presented in the previous chapters of this report. Both the solution using IMUs and using potentiometer will be discussed, followed by a suggestion of future development of the device. Finally, the ethical aspects will be presented followed by the conclusions that could be drawn from this project.

## 8.1 IMU

In the beginning of this project, the impression was that it would be easy to implement an angle measurement algorithm for IMUs. Several scientific articles presented works that investigated the usability for IMU systems for joint angle measurements. Initially, the majority of these articles were positive towards implementing IMUs but in the end many concluded that the ability for IMUs to measure movement is limited and that algorithms for doing so are complicated to implement practically.

One obstacle that occurred from using several IMUs is the difficulty of relating their different local body orientations to each other and to a global body orientation system. Other obstacles to consider are gimbal lock, the effect that magnetic fields have on IMUs and last but not least, using Euler equations for calculating joint angles when the contributions from gravity to the IMU axes are constant. When implementing the IMUs in this project, the last-mentioned obstacle appeared when simulating situations where a person has two IMUs placed on the anterior side of the leg and the person is lying on his/her side. In such a situation, the impact from gravity is constant resulting in the system being unable to record any angle changes.

Whenever the two IMUs are situated and/or moving neither in the global XY-plane nor in the global XZ-plane but instead somewhere in between these planes, a combination of different Euler angles needs to be used for estimating the joint angle.

However, finding relationships between the different Euler angles and when to implement them proved to be difficult and laborious. It became time-consuming to identify and implement different weight functions and challenging to ensure that they worked accurately and consistently for different conditions, i.e. for different positions of the leg and different flexion/extension angles. Instead the idea of using Euler equations was abandoned and a solution using a potentiometer was implemented. If having more time, finding a solution to the last-mentioned problem would have been more thoroughly explored.

Using quaternions and the dot product formula for calculating the angle between two IMUs was an interesting approach because of the quaternion vectors enabling a straightforward implementation of the dot product formula. Furthermore, no consideration had to be taken as to in which plane the angular movements happened, meaning that no weight functions had to be implemented. Initially, this approach seemed very promising since it enabled measuring the angle between two extremities regardless of their position and rotation in space. One obstacle with the dot product formula and the quaternion vectors is that if the two IMUs do not have the same tilt on their xy-plane, for instance if one the IMUs is positioned awry on the leg compared to the other, then the calculated angle will not represent the actual flexion or extension angle. At first, the perception was that such tilt would not be big enough to have a large impact on the calculated angle. However, this was not the case. A small difference in tilt between the two IMUs xy-plane had a substantial effect on the output, resulting in an highly inaccurate angle. Because of this obstacle, it would have been beneficial to implement an algorithm for continuous adjustment of the quaternions so that they always corresponded to close to identical tilt in xy-plane. An attempt to implement such an algorithm was made but without success.

Quaternions turned out to be much more difficult to use and implement than initially perceived. Information on how to accurately use quaternions was sought after in literature, Arduino web forums and from personnel at the Lund University Faculty of Engineering but little usable information was acquired. Since the approach with the dot product angle also required doubling the calculated angle, which resulted in a twice as big error, the idea of using IMUs in this project became less and less interesting.

One large problem with IMUs is that they are highly sensitive to magnetic fields, even such weak magnetic fields as from computer displays or smartphones affects the different output parameters. Originally, the impression was that a magnetic field would only affect the magnetometer in the IMU. After observing the different outputs for pitch (using outputs from the accelerometer and gyroscope), heading (using output from magnetometer), dot product angle (using quaternion

outputs), while moving the IMUs closer to a smartphone or computer display, it became evident that those magnetic fields not only affected the magnetometer. A large problem with this is that when testing different solutions in this project, the development had to be made in connection to computers. Hence, any calibration to the IMUs developed during those circumstances could become wrong in other surroundings. In other words, the accuracy of the different solutions is uncertain.

When analyzing the printed data the authors looked for accurate and promising results. Whenever the data was unstable and unreliable alterations were made before saving figures that illustrated the problem. Since the data also was so inconsistent, little was saved for further analysis. This inconsistent data is something that would have been usable for visualizing the problems and obstacles of the IMU, but was not something that was considered usable during the ongoing work.

## 8.2 Potentiometer

By implementing a potentiometer instead of the IMUs it was possible to obtain the angle of the knee joint without having to consider several body coordinate systems. In Tardieu et al, a potentiometer was implemented to measure ankle angles during 24 hours and a similar solution was created in this project, but for measuring the angle of the knee joint. Furthermore, since a potentiometer has a one-dimensional output, no weight functions needed to be implemented. The data from the potentiometer was accurate and easy to analyze compared to the IMU sensor and a wireless and wearable device could be developed from the solution.

A sample rate of 2 Hz was too low to accurately depict gait patterns. Therefore, a higher sample rate is needed if wanting to measure a dynamic and cyclic movement. If more stationary situations are to be recorded, for example during sleep, a low sample rate can be used.

One negative aspect with the potentiometer solution was that the collected measurements indicated a slight hindering of movement when wearing the device. This could be due to the knee pad being attached too tightly and stiffening the leg. This was necessary because the splints needed to be fixated to the leg to measure the movement as accurately as possible. The knee pad used in this project was the thinnest one available considering the time limit and budget, and that still was durable and did not slide around on the leg.

Another aspect of the knee pad was that when the knee was bent in more extreme angles, such as when measuring during a squat, one could clearly observe that the splints did not completely follow the movement of the leg. This could be due to the splints being too long and wide and not attached properly onto the leg. Even

though the splints did not follow the leg exactly, the gait data obtained from the device was still usable and close to the reference values.

The battery life of the device was considered satisfying and the size of the wireless components was considered small enough. However, the compartment used for holding the components was a temporary solution and is something that could easily be improved by 3D-printing a more suitable one. It was possible to remove and plug in the SD card without needing to open the compartment but when the battery need to be charged one needs to open it and connect it to a computer. This task is considered easy and can be done by either the physician or the physiotherapist, or the parent to the child.

The final prototype was considered successful as it was able to measure the angles during a longer period of time. The focus of the project was changed to the potentiometer after half of the project time had passed. This is an aspect that needs to be considered, if there had been more time the prototype could have been further developed and tested on children. The final prototype in this project is fitted for adults and therefore not suitable for children. This could easily be changed by fitting the device onto a smaller knee pad. But due to the fact that the device has not been tried on children there is no way of telling if children will be able to wear the device for a longer period of time, without taking it of.

### **8.3 Future development**

The final prototype in this project has many aspects of improvement. When changing the focus from IMU to potentiometer, some of the lightness and size of the device disappeared. The solution with the potentiometer needs to be fixated in the rotational center and the splints need to be attached to the leg so it follows the movements of the leg more accurate. As mentioned in the previous section the final prototype worked well but there was some indications that the device hindered the natural movement of the leg. An idea for future development would be to consider using a smaller potentiometer. It would also be preferable to use smaller splints and attach the device to the knee where it would have minimal impact on the natural movement.

The initial idea was to create a device that worked on both the knee and the ankle. Developing a device that would interfere as little as possible with the movements is probably easier when using the IMU solution rather than using the potentiometer. This is because the potentiometer device would likely be too cumbersome. However, the device in Tardieu et al was, as mentioned previously, used for ankle measurements. The article states that "The equipment was designed so that it did



not hinder spontaneous movements in eversion or inversion", and that it enabled measuring ankle angles throughout 24 hours of a child's ordinary life. Nonetheless, the measurement was of the ankle flexion angle (dorsiflexion and plantar flexion) and not the eversion/inversion angle and it is uncertain how much the device interfered with flexion since the arms of the potentiometer were fixed to leg and hindfoot castings.

Another aspect would be to investigate the possibility to measure on both legs at the same time. This could increase the possibility of finding variations in the movement pattern of the child.

The device has not been tested on children during this project. This is something important to consider in further development, both the technical and ergonomic aspects. The device need to accurately measure the range of motion children as it was able to measure on adults. It is also important that the device is comfortable for the child to wear and not interfere with the daily life. The most ideal scenario would be if the child completely forgets about the device when it is attached to the leg. That would give the most accurate measurement and would be best for the child.

## **8.4 Ethical aspects**

Children that are diagnosed with Cerebral Palsy often suffer from complications during their growth. It is common that they have higher tension in some muscles while other muscles are impaired. This imbalance can lead to shortening of some muscles which can cause contractures and joint dislocation and scoliosis. This is very painful for the child and affects the quality of life for the rest of one's life. It is important that measures to prevent this are introduced early in the child's life.

By having continuous follow-ups and early treatment, these children can achieve optimal function in the body parts affected by CP. The understanding and knowledge in the area of CP can also increase by treating the children early.

Today the physiotherapist or occupational therapist evaluate the child during a short examination of the movement and function of several joints. The device that has been developed in this project is able to measure the range of movement of the joints during a longer period of time. The expectation is that this device might be a help when evaluating children with CP and and a way to better customize the treatment.

The device that was developed in this project has not yet been tested on children. The development has solely been tested and evaluated on the project members.

The reason for this was mainly due to the time limit in this project but also because there was an uncertainty to if there was a need for an ethical approval.

When continuing with developing this device and testing it on children with CP there is a need for performing an ethical review. There are numerous factors to take into consideration. For instance, it is important that the use of the device does not cause the child to feel anxious, uncomfortable or distressed.

## **8.5 Conclusions**

It is possible to measure the range of motion of a knee by using a potentiometer. Inertial measurement units are a possibility in developing a more lightweight measurement solution but it is very complex and the measurements are inaccurate. To implement a solution using IMU, one needs more time and knowledge to understand the complexity of the sensors.

## 9 | References

- [1] L. Mutch, E. Alberman, B. Hagberg, K. Kodama, and M. V. Perat, “Cerebral palsy epidemiology: Where are we now and where are we going?”, *Developmental medicine and child neurology*, vol. 34, no. 6, pp. 547–551, Jun. 1992.
- [2] M. L. Aisen, D. Kerkovich, J. Mast, S. Mulroy, T. A. Wren, R. M. Kay, and S. A. Rethlefsen, “Cerebral palsy: Clinical care and neurological rehabilitation”, *The Lancet Neurology*, vol. 10, no. 9, pp. 844–852, Sep. 2011.
- [3] N. I. of Neurological Disorders and P. L. Stroke (US) Office of Communications and, *Cerebral Palsy: Hope Through Research*. National Institute of Neurological Disorders and Stroke, National Institutes of Health, 2009.
- [4] R. H. Widmayer EP and S. KT, *Vander’s Human Physiology: The Mechanisms of Body Function*. McGraw-Hill, 2016, vol. 14th edition.
- [5] M. Hermanson, “Prevention of hip dislocation in children with cerebral palsy”, PhD dissertation, Lund University, Faculty of Medicine, 2017.
- [6] *Cpup - uppföljningsprogram för cerebral pares*, retrieved 11/10, 2017. [Online]. Available: [cpup.se/vad-ar-cp/](http://cpup.se/vad-ar-cp/).
- [7] *Gunnar hägglund*, Personal interview, Oct. 2017.
- [8] M. Oskoui, F. Coutinho, J. Dykeman, N. Jetté, and T. Pringsheim, “An update on the prevalence of cerebral palsy: A systematic review and meta-analysis”, *Developmental Medicine Child Neurology*, vol. 55, no. 6, pp. 509–519, 2013.
- [9] E. Rodby Bousquet, “Posture, postural ability and mobility in cerebral palsy”, PhD dissertation, Lund University, Faculty of Medicine, 2012.
- [10] C. Cans, “Surveillance of cerebral palsy in europe: A collaboration of cerebral palsy surveys and registers”, *Developmental Medicine Child Neurology*, vol. 42, no. 12, pp. 816–824, 2000.

## References

---

- [11] K. W. Nolan, L. L. Cole, and G. S. Liptak, “Use of botulinum toxin type a in children with cerebral palsy”, *Physical Therapy*, vol. 86, no. 4, pp. 573–584, 2006.
- [12] *Fass, baklofen*, retrieved 28/9, 2017. [Online]. Available: <http://www.fass.se/LIF/product?userType=0&nplId=20100930000058>.
- [13] J. D. Bronzino and J. D. Enderle, *Introduction to biomedical engineering*, 3. ed. Amsterdam: Elsevier, Acad. Press, 2012, pp. 120–121, ISBN: 0123749794.
- [14] G. J. Betts, P. Desaix, E. Johnson, J. E. Johnson, O. Korol, D. Kruse, B. Poe, J. A. Wise, M. Womble, and K. A. Young, *Anatomy and Physiology*. OpenStax, 2013, pp. 365–367. [Online]. Available: <https://openstax.org/details/books/anatomy-and-physiology>.
- [15] P. Adam, *Guide to knee joint anatomy*, Nov. 2015. [Online]. Available: <https://www.sports-health.com/sports-injuries/knee-injuries/guide-knee-joint-anatomy>.
- [16] Medical gallery of Blausen Medical 2014. WikiJournal of Medicine 1 (2). DOI:10.15347/wjm/2014.010. ISSN 2002-4436. [Online]. Available: Blausen.com.
- [17] Movement of the knee. Msk-anatomyblogspotse. 2014, retrieved 11/1, 2018. [Online]. Available: <http://msk-anatomy.blogspot.se/2014/08/movement-of-knee.html>.
- [18] P. contributors, *Physiopedia*, retrieved 10/1, 2018. [Online]. Available: <https://www.physio-pedia.com/index.php?title=Knee&oldid=181449>.
- [19] F. V. Nordin M, *Basic Biomechanics Of The Musculoskeletal System*. Philadelphia: Wolters Kluwer Health/Lippincott Williams Wilkins, 2012.
- [20] M. McKay, J. Baldwin, P. Ferreira, M. Simic, N. Vanicek, and J. Burns, “Normative reference values for strength and flexibility of 1,000 children and adults”, *Neurology*, vol. 88, no. 1, pp. 36–43, 2016.
- [21] J. M. Soucie, C. Wang, A. Forsyth, S. Funk, M. Denny, K. E. Roach, and D. Boone, “Range of motion measurements: Reference values and a database for comparison studies”, *Haemophilia*, vol. 17, no. 3, pp. 500–507, May 2011.
- [22] R. D. Tugui and D. Antonescu, “Cerebral palsy gait, clinical importance”, *Maedica*, vol. 8, no. 4, pp. 388–393, 2013.
- [23] H. Böhm, M. Hösl, H. Schwameder, and L. Döderlein, “Stiff-knee gait in cerebral palsy: How do patients adapt to uneven ground?”, *Gait Posture*, vol. 39, no. 4, pp. 1028–1033, 2014.

- 
- [24] F. Bilgili, Y. Temelli, and N. E. Akalan, “Assessment of the hip and knee flexion contractures in cerebral palsy patients with crouch gait”, vol. 2, pp. 10–14, Nov. 2012.
- [25] P. contributors, *Flexion deformity of the knee*, retrieved 10/1, 2018. [Online]. Available: [https://www.physio-pedia.com/index.php?title=Flexion\\_Deformity\\_of\\_the\\_Knee&oldid=178168](https://www.physio-pedia.com/index.php?title=Flexion_Deformity_of_the_Knee&oldid=178168).
- [26] *Cerebral palsy, orthotics*, retrieved 18/11, 2017. [Online]. Available: <http://www.cerebralpalsy.org/information/mobility/orthotics>.
- [27] *Sparkfun hookup guide - lsm9ds1*, retrieved 13/11, 2017. [Online]. Available: <https://learn.sparkfun.com/tutorials/lsm9ds1-breakout-hookup-guide>.
- [28] *Wolfram mathworld, euler angles*, retrieved 10/12, 2017. [Online]. Available: <http://mathworld.wolfram.com/EulerAngles.html>.
- [29] F. Abyarjoo, A. Barreto, J. Cofino, and F. R. Ortega, “Implementing a sensor fusion algorithm for 3d orientation detection with inertial/magnetic sensors”, T. Sobh and K. Elleithy, Eds., pp. 305–310, 2015.
- [30] O. Woodman, “An introduction to inertial navigation, technical report”, 2007.
- [31] *Compass heading using magnetometers, honeywell*, retrieved 28/9, 2017. [Online]. Available: [https://aerocontent.honeywell.com/aero/common/documents/myaerospacecatalog-documents/Defense\\_Brochures-documents/Magnetic\\_Literature\\_Application\\_notes-documents/AN203\\_Compass\\_Heading\\_Using\\_Magnetometers.pdf](https://aerocontent.honeywell.com/aero/common/documents/myaerospacecatalog-documents/Defense_Brochures-documents/Magnetic_Literature_Application_notes-documents/AN203_Compass_Heading_Using_Magnetometers.pdf).
- [32] *Hoffmann, g., infamous gimbal lock, 2002*, retrieved 30/11, 2017. [Online]. Available: <http://docs-hoffmann.de/gimbal09082002.pdf>.
- [33] MathsPoetry, (Own work) GFDL license at <http://www.gnu.org/copyleft/fdl.html>, retrieved 23/1, 2018. [Online]. Available: [https://upload.wikimedia.org/wikipedia/commons/c/c4/No\\_gimbal\\_lock.png](https://upload.wikimedia.org/wikipedia/commons/c/c4/No_gimbal_lock.png).
- [34] MathsPoetry, (Own work) GFDL license at <http://www.gnu.org/copyleft/fdl.html>, retrieved 23/1, 2018. [Online]. Available: [https://upload.wikimedia.org/wikipedia/commons/3/38/Gimbal\\_lock.png](https://upload.wikimedia.org/wikipedia/commons/3/38/Gimbal_lock.png).
- [35] *Ch robotics, understanding quaternions*, retrieved 30/11, 2017. [Online]. Available: <http://www.chrobotics.com/library/understanding-quaternions>.
- [36] J. Vince, *Quaternions for Computer Graphics*. Springer-Verlag London Limited, 2011, pp. 89–101.
- [37] *Random nerd tutorials, electronics basics – how a potentiometer works*, retrieved 30/11, 2017. [Online]. Available: <https://randomnerdtutorials.com/electronics-basics-how-a-potentiometer-works/>.
-

- [38] *Wikipedia, potentiometer*, retrieved 30/11, 2017. [Online]. Available: <https://sv.wikipedia.org/wiki/Potentiometer>.
- [39] Retrieved 16/1, 2018. [Online]. Available: [https://media.rs-online.com/t\\_large/F0387745-01.jpg](https://media.rs-online.com/t_large/F0387745-01.jpg).
- [40] *Arduino*, retrieved 28/9, 2017. [Online]. Available: <https://www.arduino.cc/>.
- [41] B. Tonnquist, *Projektledning*. Sanoma Utbildning, 2016.
- [42] K. Ulrich and S. Eppinger, *Product Design and Development*, 4th. McGraw-Hill Education/Asia, 2011.
- [43] C. Tardieu, A. Lesparget, C. Tabart, and M. D. Bret, “For how long must the soleus muscle be stretched each day to prevent contracture?”, *Developmental Medicine and Child Neurology*, vol. 30, pp. 3–10, 1988.
- [44] *Research methodology, snowball sampling*, retrieved 28/9, 2017. [Online]. Available: <https://research-methodology.net/sampling-in-primary-data-collection/snowball-sampling/>.
- [45] S. A., “Tips and tricks in performing a systematic review.”, *Br J Gen Pract.*, vol. 57, no. 538, p. 425, 2006.
- [46] R. McLaren, F. Joseph, C. Baguley, and D. Taylor, “A review of e-textiles in neurological rehabilitation: How close are we?”, *Journal of neuroengineering and rehabilitation*, vol. 13, no. 1, p. 59, 2016.
- [47] A. Tognetti, F. Lorussi, G. D. Mura, N. Carbonaro, M. Pacelli, R. Paradiso, and D. D. Rossi, “New generation of wearable goniometers for motion capture systems”, *Journal of neuroengineering and rehabilitation*, vol. 11, p. 56, 2014.
- [48] *Lubsearch*, retrieved 16/1, 2018. [Online]. Available: <https://www.lubsearch.lub.lu.se>.
- [49] N. P. Oess, J. Wanek, and A. Curt, “Design and evaluation of a low-cost instrumented glove for hand function assessment”, *Journal of neuroengineering and rehabilitation*, vol. 9, no. 1, p. 2, 2012.
- [50] S. Patel, H. Park, P. Bonato, L. Chan, and M. Rodgers, “A review of wearable sensors and systems with application in rehabilitation”, *Journal of neuroengineering and rehabilitation*, vol. 9, no. 1, p. 21, 2012.
- [51] N. Carbonaro, G. D. Mura, F. Lorussi, R. Paradiso, D. D. Rossi, and A. Tognetti, “Exploiting wearable goniometer technology for motion sensing gloves”, *IEEE Journal of Biomedical and Health Informatics*, vol. 18, no. 6, pp. 1788–1795, 2014.

- 
- [52] S. J. Preece, L. P. J. Kenney, M. J. Major, T. Dias, E. Lay, and B. T. Fernandes, “Automatic identification of gait events using an instrumented sock”, *Journal of neuroengineering and rehabilitation*, vol. 8, no. 1, p. 32, 2011.
- [53] T.-W. Shyr, J.-W. Shie, C.-H. Jiang, and J.-J. Li, “A textile-based wearable sensing device designed for monitoring the flexion angle of elbow and knee movements”, *Sensors (Basel, Switzerland)*, vol. 14, no. 3, pp. 4050–4059, 2014.
- [54] P. Picerno, A. Cereatti, and A. Cappozzo, “Joint kinematics estimate using wearable inertial and magnetic sensing modules”, *Gait Posture*, vol. 28, no. 4, pp. 588–595, 2008.
- [55] H. Lau and K. Tong, “The reliability of using accelerometer and gyroscope for gait event identification on persons with dropped foot”, *Gait Posture*, vol. 27, no. 2, pp. 248–257, 2008.
- [56] C.-M. Yang, Z.-S. Lin, C.-L. Hu, Y.-S. Chen, L.-Y. Ke, and Y.-R. Chen, “A novel dynamic sensing of wearable digital textile sensor with body motion analysis”, vol. 2010, pp. 4898–4901, 2010.
- [57] M. Sung, K. Jeong, and G. Cho, “Establishing a measurement system for human motions using a textile-based motion sensor”, pp. 784–792, Jul. 2009.
- [58] B. C. McDowell, V. Hewitt, A. Nurse, T. Weston, and R. Baker, “The variability of goniometric measurements in ambulatory children with spastic cerebral palsy”, *Gait Posture*, vol. 12, no. 2, pp. 114–121, 2000.
- [59] J. C. van den Noort, V. A. Scholtes, and J. Harlaar, “Evaluation of clinical spasticity assessment in cerebral palsy using inertial sensors”, *Gait Posture*, vol. 30, no. 2, pp. 138–143, 2009.
- [60] P. Herrero, P. Carrera, E. García, E. Gómez-Trullén, and B. Oliván-Blázquez, “Reliability of goniometric measurements in children with cerebral palsy: A comparative analysis of universal goniometer and electronic inclinometer. a pilot study”, vol. 12, p. 155, Jul. 2011.
- [61] S. Choi and J. Kim, *Improving modified tardieu scale assessment using inertial measurement unit with visual biofeedback*. 2016.
- [62] X. Chen, S. Liao, S. Cao, D. Wu, and X. Zhang, “An acceleration-based gait assessment method for children with cerebral palsy”, *Sensors (Basel, Switzerland)*, vol. 17, no. 5, 2017, ISSN: 1424-8220.
- [63] A. B. Bourgeois, B. Mariani, K. Aminian, P. Zambelli, and C. Newman, “Spatio-temporal gait analysis in children with cerebral palsy using, foot-worn inertial sensors”, *Gait Posture*, vol. 39, no. 1, pp. 436–442, 2014, ISSN: 0966-6362.
-

- [64] A. G. Cutti, A. Ferrari, P. Garofalo, M. Raggi, A. Cappello, and A. Ferrari, “‘outwalk’: A protocol for clinical gait analysis based on inertial and magnetic sensors”, *Medical & Biological Engineering & Computing*, vol. 48, no. 1, p. 17, 2009.
- [65] T. Seel, J. Raisch, and T. Schauer, “Imu-based joint angle measurement for gait analysis”, vol. 14, pp. 6891–909, Apr. 2014.
- [66] H. Nwaizu, R. Saatchi, and D. Burke, *Accelerometer based human joints’ range of movement measurement*. 2016, pp. 1–6.
- [67] *Arduino software*, retrieved 16/9, 2017. [Online]. Available: <https://www.arduino.cc/en/Main/Software>.
- [68] I. Frosio, F. Pedersini, and N. A. Borghese, “Autocalibration of mems accelerometers”, *IEEE Transactions on Instrumentation and Measurement*, vol. 58, no. 6, pp. 2034–2041, 2009.
- [69] *Coolterm software*, retrieved 20/10, 2017. [Online]. Available: <http://freeware.the-meiers.org/>.
- [70] *Adafruit 9-dof absolute orientation imu fusion breakout - bno055*, retrieved 13/11, 2017. [Online]. Available: <https://www.adafruit.com/product/2472>.
- [71] O. College, *Introductory statistics OpenStax College*. OpenStax College, 2015, pp. 540–541. [Online]. Available: <http://cnx.org/content/col11776/latest>.
- [72] P. C. Bruce, *Introductory Statistics and Analytics: A Resampling Perspective*. John Wiley Sons, 2015, p. 262.
- [73] B. Scrosati, K. M. Abraham, W. A. van Schalkwijk, and J. H. (ed), *Batteries: Advanced Technologies and Applications*, J. W. Sons, Ed. 2013, p. 44.
- [74] *Arduino, millis()*, retrieved 13/11, 2017. [Online]. Available: <https://www.arduino.cc/reference/en/language/functions/time/millis/>.
- [75] W.-Y. Chen and C.-S. Lin, “A study of the influence from different running slope on the angles of limb joints”, in *31st International Conference on Biomechanics in Sports*. 2013.
- [76] *Kinovea*, retrieved 8/1, 2018. [Online]. Available: <https://www.kinovea.org/>.